



**HAL**  
open science

## Stimuli-Responsive Toughening of Hydrogels

Xinxing Lin, Xiaolin Wang, Liangpeng Zeng, Zi Liang Wu, Hui Guo,  
Dominique Hourdet

► **To cite this version:**

Xinxing Lin, Xiaolin Wang, Liangpeng Zeng, Zi Liang Wu, Hui Guo, et al.. Stimuli-Responsive Toughening of Hydrogels. *Chemistry of Materials*, 2021, 10.1021/acs.chemmater.1c01019 . hal-03346113

**HAL Id: hal-03346113**

**<https://espci.hal.science/hal-03346113>**

Submitted on 16 Sep 2021

**HAL** is a multi-disciplinary open access archive for the deposit and dissemination of scientific research documents, whether they are published or not. The documents may come from teaching and research institutions in France or abroad, or from public or private research centers.

L'archive ouverte pluridisciplinaire **HAL**, est destinée au dépôt et à la diffusion de documents scientifiques de niveau recherche, publiés ou non, émanant des établissements d'enseignement et de recherche français ou étrangers, des laboratoires publics ou privés.



14 ABSTRACT

15 Materials with stimuli-switchable properties are widespread in nature. Through  
16 biomimicry, stimuli-responsive hydrogels have received increasing research in recent  
17 years. In particular, hydrogels with stimuli-tunable mechanical properties provide an  
18 important platform for designing new materials with specific applications such as 3D  
19 printing, soft robot, and tunable adhesion. Herein, the state-of-the-art of hydrogels with  
20 stimuli-responsive toughness is reviewed in detail. Characteristic reinforcement  
21 mechanisms are fully discussed first, followed by systematical demonstrations of various  
22 smart hydrogels responding to various stimuli. In particular, special attention is paid to  
23 thermal, light, pH, and salt triggers because of their broad applications and easy  
24 implementation. Furthermore, the applications of these smart hydrogels are included. In  
25 addition to the overview of recent advances, we finally summarize the critical challenges  
26 of current discoveries and make an outlook for the following work, which we anticipate to  
27 lead to substantial progress of these responsive materials in the future.

28

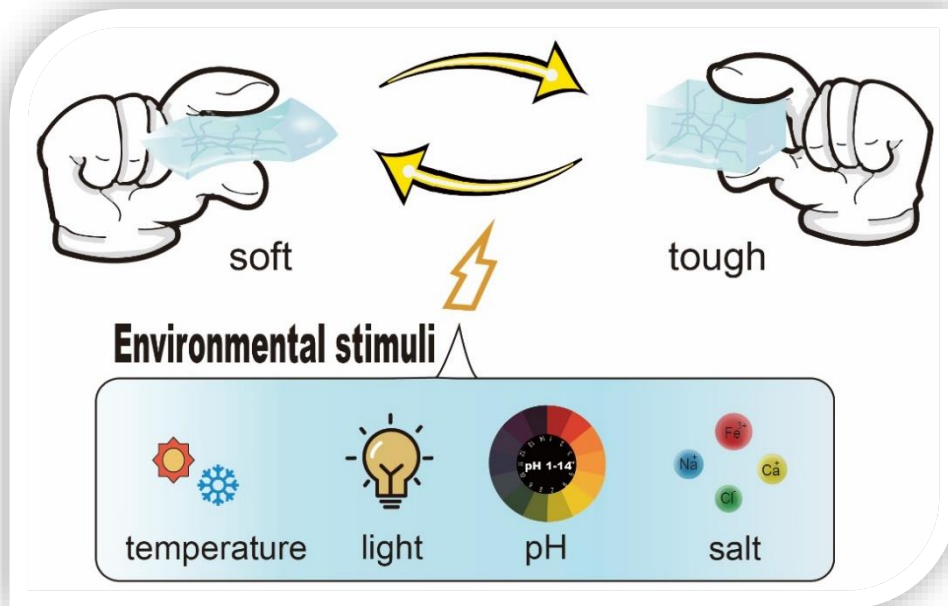
## 29 **Introduction**

30 Living materials consist of various smart components whose performance can be finely  
31 tuned by stimuli. For instance, muscles reversibly stiffen or soften in response to neutral  
32 signals, chameleons hold the ability to change color in response to several environmental  
33 triggers, and Mimosa Pudica leaves close automatically under mechanical disturbances.  
34 Learning from nature, bio-inspired materials with stimuli-responsiveness have attracted  
35 considerable attention during the last few decades.<sup>1</sup> In particular, stimuli-responsive  
36 hydrogels, which are often termed as smart hydrogels, have been intensively investigated  
37 as they automatically respond to environmental changes.<sup>2-3</sup> Bearing high level of water  
38 contents, hydrogels serve as ideal candidates for bio-engineering applications as they share  
39 versatile similarities with human tissues.<sup>4-5</sup> Moreover, their ability to be programmed  
40 concerning one or various given stimuli considerably broadens their application  
41 perspectives. Typical stimuli involve temperature, pH, humidity, light, specific ions or  
42 molecules, electrical field, magnetic field, solvent, and ionic strength. Therefore, these  
43 smart hydrogels demonstrate great potential for developing specific applications, from  
44 targeted drug delivery<sup>6</sup> to precisely controlled actuators,<sup>7-8</sup> from artificial muscles<sup>9</sup> to self-  
45 healable tissue,<sup>10</sup> and from photochromic windows<sup>11</sup> to magnetic sensors.<sup>12</sup>

46 When subjected to external stimuli, the response of hydrogels is transmitted from the  
47 microscopic level to the macroscopic scale. Their optical transparency is easily tunable,  
48 their size and shape are readily controllable, and their hydrophilicity is finely adjustable.<sup>13</sup>

49 Apart from these features, smart hydrogels can also demonstrate switchable mechanical  
50 performance, with dramatic modifications of their rigidity, extensibility, and toughness.  
51 Therefore, these hydrogels are able to adapt to complex environments and can be used in  
52 relevant applications where stimuli-tunable soft materials are required. For example, a soft  
53 robot needs the mechanical responsiveness of its components in order to accomplish a  
54 complex movement.<sup>14</sup>

55 While stimuli-responsive hydrogels have already been adequately addressed and fully  
56 summarized based on their tunable size,<sup>15</sup> color,<sup>16</sup> and even electro-conductivity,<sup>2</sup> the  
57 control of their mechanical properties by environmental stimuli has been much less  
58 investigated and rationalized. To fill this gap, recent advances in the field of three-  
59 dimensional hydrogels with stimuli-responsive toughness are highlighted and summarized  
60 in this review (Figure 1). Associating polymer solutions that undergo sol-gel transition and  
61 form transient unstable weak networks are excluded from the discussion. In the first part,  
62 the different mechanisms involved in the viscoelastic response of hydrogels are carefully  
63 discussed before describing the main stimuli used to modify their mechanical performances.  
64 Special attention is given to thermal, light, pH, and salt responsive hydrogels. The  
65 responsive mechanical properties of hydrogels are explored and both the advantages and  
66 weaknesses of these smart systems are discussed. Finally, this review provides concluding  
67 remarks over the recent advances and challenges in this field with some guiding ideas  
68 which could inspired new findings.



69

70 **Figure 1. Schematic illustration of hydrogels with stimuli-responsive mechanical performance.**

71

72 **1. Mechanisms of hydrogels with responsive mechanical performance**

73 Before discussing the stimuli-responsiveness, it is important to briefly recall some basic  
 74 elements relating to the viscoelastic properties of hydrogels, typically the elastic and  
 75 dissipative behaviors. Hydrogels are soft materials composed of crosslinked polymer  
 76 chains typically swollen with water. While absorbing a large amount of solvent inside the  
 77 three-dimensional network with osmotic pressure contribution, hydrogels still maintain  
 78 solid-state with certain levels of mechanical performance. The swelling and elasticity of  
 79 hydrogels are directly related to the crosslink density of the network, its polymer volume  
 80 fraction as well as the interactions between solvent and polymer. According to the classical

81 theory of rubber elasticity,<sup>17-18</sup> the shear modulus  $G$  of swollen hydrogel having no  
82 permanent (trapped) entanglements can be described by the relation below,

$$83 \quad G \cong kTv_{e,\phi} = \frac{RT\rho_0\phi_0^a\phi^b}{M_0N} \quad (1)$$

84 with  $v_{e,\phi}$  the number density of elastically active chains at the polymer volume fraction  $\phi$ ,  
85  $k$  the Boltzmann constant,  $R$  the gas constant,  $T$  the temperature,  $\phi_0$  the polymer volume  
86 fraction in the preparation state,  $\rho_0$  the polymer density,  $M_0$  the molar mass of the monomer,  
87 and  $N$  the number of monomers per elastic strand. In equation (1),  $a$  and  $b$  are scaling  
88 exponents which depend on the quality of the solvent ( $a = 2/3$ ,  $b = 1/3$  in  $\theta$  conditions and  
89  $a = 5/12$ ,  $b = 7/12$  in a good solvent), with  $G \sim \phi_0$  for gels in the preparation state ( $\phi = \phi_0$ ).  
90 From equation (1), we can see that the polymer volume fraction, the quality of solvent, and  
91 the molar mass between crosslinks determine the elastic modulus for a given hydrogel.  
92 This concentration dependence is valid for chemical networks having no permanent  
93 (trapped) entanglements which means that  $N$  is shorter than the length of an entanglement  
94 strand at the preparation concentration  $N_e(\phi_0)$ . In the opposite situation,  $N_e(\phi_0) < N$ , the  
95 elastic properties are dominated by entanglements and  $G \sim RT\phi_0^c\phi^d$  ( $c = 2$ ,  $d = 1/3$  in  $\theta$   
96 conditions and  $c = 5/3$ ,  $d = 7/12$  in a good solvent); with  $G \sim \phi_0^{2.3}$  for gels in the preparation  
97 state.<sup>18</sup> All these equations derived from linear elasticity, assuming Gaussian statistics for  
98 polymer chains, hold at low deformation. This is no longer the case when the chains are  
99 subjected to larger deformations where more sophisticated statistical approaches may be

100 used, like Langevin statistics<sup>19</sup> to model the nonlinear rubber elasticity. This is the case for  
101 highly swollen polyelectrolyte networks which become stiffer ( $G$  increases) when the  
102 chains are stretched with the swelling ( $v_{e,\phi}$  decreases).<sup>20</sup>

103 While the stiffness of swollen polymer networks is something relatively well understood  
104 and quite easily controlled, hydrogels remain fragile materials. Indeed, they are  
105 characterized by low mechanical properties in terms of extensibility and tenacity which are  
106 currently a hot topic in the scientific community of hydrogels. Experimentally, the  
107 measured strain and stress at break of material correspond to the point where a crack  
108 propagates through the sample. Therefore, we can assume, as proposed by Maugis and  
109 Barquins,<sup>21</sup> that the interfacial fracture energy  $\Gamma(v)$  can be empirically written as:

$$110 \quad \Gamma(v) = \Gamma_0(1 + f(a_T v)) \quad (2)$$

111 where  $f(a_T v)$  is a velocity-dependent dissipative factor with  $v$  the crack velocity and  
112  $a_T$  the time-temperature superposition shift factor;  $\Gamma_0$  is the threshold fracture energy for  
113 vanishing crack velocities, mostly related to the chemistry of the interface. Based on the  
114 molecular theory for  $\Gamma_0$  developed by Lake *et al.*,<sup>22</sup> when any of the main chain bonds break,  
115 the total bond energy of each bond of the stretched chain is irreversibly lost. Therefore, the  
116 minimum energy necessary to break the chain is proportional to the length of that chain,  
117 *i.e.*, to the number of C-C bonds comprising that  $N$ -chain. Assuming that only the strands  
118 crossing the fracture plane will break for a homogeneously crosslinked hydrogel,  $\Gamma_0$  can be

119 written as:<sup>22-23</sup>

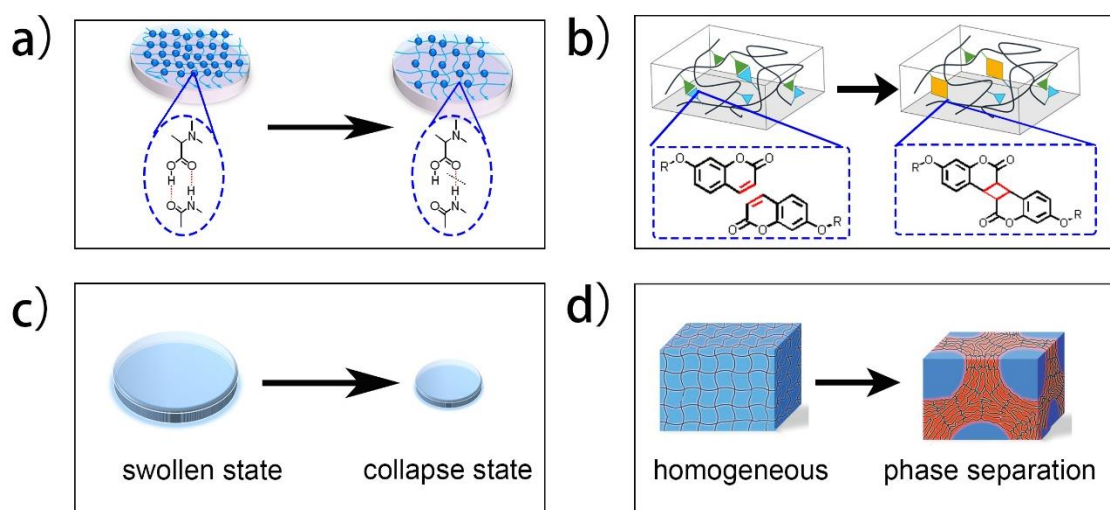
$$120 \quad \Gamma_0 = NU_b\Sigma \approx U_b v_{e,\varphi=1} \phi a N^{\frac{3}{2}} \approx \frac{U_b a \rho_0 \phi}{M_0} N^{\frac{1}{2}} \quad (3)$$

121 where  $\Sigma$  is the areal density of strands crossing the interface,  $U_b$  is the bond energy of a C-  
122 C bond ( $\sim 350$  kJ/mol),  $v_{e,\varphi=1}$  the number density of elastically active chains in the melt  
123 state and  $a$  is the size of the monomer. From this equation, it turns out that the fracture  
124 energy of hydrogels is also related to their polymer volume fraction and crosslinking  
125 density, though the dependence is distinct from that on elastic shear modulus. Indeed, the  
126 crosslinking density, which is directly related to reciprocal  $N$ , is positively related to  $G$  but  
127 negatively contributes to  $\Gamma$ . Consequently, there is a trade-off between rigidity and  
128 toughness. In contrast, both  $G$  and  $\Gamma$  demonstrate a consistent relationship to  $\phi$ , which  
129 means that both rigidity and toughness decrease when the gel swells; i.e.  $\phi$  decreases.

130 Based on equation (2), the velocity-dependent dissipative factor  $f(a_T v)$  also plays an  
131 important role in determining hydrogels' toughness. This factor, which considers the  
132 mechanical dissipation in the bulk, is related to the crack velocity  $v$  and the time-  
133 temperature superposition shift factor  $a_T$ . Along with the crack propagation velocity, the  
134 rise of molecular friction and noncovalent interactions between polymer chains increase  
135 dissipation processes and these effects have been clearly shown to significantly increase  
136 the fracture energy of soft materials.<sup>24-25</sup> For water-swollen hydrogels, which are generally  
137 characterized by a low polymer volume fraction and a weak dissipative factor, physical

138 interactions<sup>26-27</sup> that can reversibly break under stretch can significantly enhance the  
139 hydrogels toughness. Moreover, the plasticity of the gel, which can be implemented by  
140 incorporating stiffer domains that can only be deformed above a certain stress level, can  
141 also greatly contribute to the hydrogel strengthening.<sup>28-29</sup>

142 Considering the above theories, the mechanical performances of hydrogels strongly depend  
143 on the crosslink density, the volume fraction, and the polymer chain interactions. By tuning  
144 these factors with external triggers, stimuli-responsive hydrogels can toughen or soften on  
145 demand. As shown in Figure 2, the typical mechanisms involve noncovalent interactions,  
146 formation or scission of covalent bonds, change in water content, phase separation, etc.



147

148 **Figure 2. Mechanisms of hydrogels with responsive toughness. a) Noncovalent interactions. b)**  
149 **Formation or scission of covalent bonds. c) Volume change. d) Phase separation. Reproduced with**  
150 **permission.<sup>30</sup> Copyright 2020 Wiley-VCH Verlag GmbH & Co. KGaA.**

151

## 152 1.1 Influence of noncovalent interactions

153 Generally, stimuli-responsive hydrogels develop various noncovalent interactions within  
154 their three-dimensional polymer networks.<sup>24, 31</sup> These noncovalent interactions includes  
155 hydrophobic interactions,<sup>32</sup> hydrogen-bonds,<sup>33</sup> dipole-dipole interactions,<sup>34</sup> coordinate  
156 bonds,<sup>35</sup> etc. These interactions may serve as dynamic bonds under stretch, thus increasing  
157 the dissipative factor and then toughening the hydrogels. When subjected to environmental  
158 signals, the strength of these physical interactions can be reversibly/irreversibly influenced.  
159 For example, hydrogen bonds are generally temperature-dependent,<sup>36</sup> the strength of  
160 coordinate bonds is often sensitive to environmental pH conditions<sup>37-38</sup> and the association  
161 between anions and cations is likely to be screened by the addition of salts.<sup>39</sup> Therefore,  
162 the application of environmental stimuli can easily lead to responsive stiffening or  
163 weakening of hydrogels.

## 164 1.2 Formation or scission of covalent bonds

165 When experiencing environmental variations, new covalent bonds may form or/and  
166 existing covalent bonds may break. Along with the formation or scission of covalent bonds,  
167 the effective crosslinking degree of hydrogels is affected and consequently its mechanical  
168 properties. This is somewhat more ubiquitous in light-responsive hydrogels, as the high  
169 energy of light is able to readily influence chemical bonds, including the cleavage,<sup>40</sup>  
170 addition,<sup>41</sup> exchange,<sup>42-43</sup> and isomerization.<sup>44-45</sup> The shape and toughness of light-sensitive

171 hydrogels can be modulated by adjusting wavelength or time of irradiation.<sup>41</sup>

### 172 1.3 Volume change

173 Both elastic and fracture behavior of hydrogel are highly affected by its water content.

174 According to the theories of rubber elasticity and Lake-Thomas<sup>46</sup> discussed previously,

175 both rigidity ( $G$ ) and toughness ( $I$ ) of hydrogels increase with the polymer volume fraction

176 ( $\phi$ ) and then decrease with the swelling of the gel ( $Q = 1/\phi = V_{sw}/V_{dry}$ ), with  $Q$  the

177 swelling ratio and  $V_{sw}$ ,  $V_{dry}$  the swollen and dry volumes of the gel. External stimuli may

178 then induce a variation of the osmotic pressure within the polymer network, giving rise to

179 water diffusion inside or outside the gel which will consequently affect its mechanical

180 properties. At the same time, large volume contractions can also induce stronger polymer

181 interactions<sup>47</sup> thus leading to further reinforcement of the hydrogels.

### 182 1.4 Phase separation

183 Upon stimuli changing the environmental conditions, water may shift from a good solvent

184 to a poor solvent for the polymer network. In such a case, the gels tend to become opaque

185 due to phase separation giving rise to an alternation of dense and sparse polymer regions

186 forming discontinuous or bicontinuous domains at the submicron scale.<sup>48-49</sup> While the rich

187 polymer phase forms a load-bearing scaffold percolating through the whole network in

188 response to the stimulus, the mechanical performances of the gel are simultaneously

189 modulated. For instance, Shibayama et al. have detailed the change of viscoelastic  
190 properties of thermo-responsive hydrogels upon phase separation.<sup>50</sup> Compared to other  
191 aforementioned mechanisms, the phase separation process has a much greater impact on  
192 the reinforcement of hydrogels. When a hydrophilic polyacrylamide hydrogel is transferred  
193 from water to a *N,N*-dimethylformamide (DMF)/water mixture, the gel undergoes rapid  
194 phase separation and demonstrates a strong improvement in stiffness, toughness, with self-  
195 healing properties and an increased elastic modulus over more than 4 decades.<sup>51</sup> A similar  
196 behavior was reported with the phase separation of *N,N*-dimethylacrylamide hydrogel  
197 induced by inorganic additives with an abrupt change of mechanical properties around the  
198 transition point.<sup>52</sup>

199 It is worthwhile mentioning that more than one mechanism may play a synergistic effect  
200 in the responsive regulation of the mechanical performances of smart hydrogels. Taking  
201 for instance thermo-responsive poly(*N*-isopropylacrylamide) hydrogel, the material is  
202 remarkably strengthened when heated above the phase transition temperature with the  
203 synergistic contribution of enhanced physical interactions, shrinkage, and phase  
204 separation.<sup>53</sup> Although the above mechanisms generally go hand in hand, it is important to  
205 stress that the phase separation phenomenon largely dominates the others. It can even lead  
206 to a mechanical reinforcement of the gel even when the latter swells during the phase  
207 separation, as recently shown in the case of organogels immersed in water.<sup>54</sup>

208 Various physical or chemical stimuli may induce toughening or weakening of hydrogels  
209 according to the mechanisms discussed above. Within the field of responsive hydrogels,  
210 thermal, light, pH, and salt stimuli were mostly investigated in the past few years although  
211 other triggers, such as magnetic<sup>55</sup> or electric fields,<sup>56-58</sup> can also be used to stimulate the  
212 mechanical properties. In the following, we will review relevant examples of smart  
213 hydrogels whose mechanical properties can be switched by different signals and discuss  
214 their characteristics in detail.

## 215 **2. Thermo-responsive hydrogels**

216 Among the possible environmental stimuli, the temperature is certainly the most widely  
217 used trigger to adjust the mechanical performance of hydrogels. Short response time, easy  
218 to operate, and adjustable transition temperatures account for its broad application.  
219 According to the toughening mechanisms, temperature-responsive, or more often termed  
220 as thermo-responsive hydrogels with stimulated mechanical performance can be classified  
221 into three main categories: hydrogels with polymer phase separation, hydrogels with  
222 glassy-like transition, and hydrogels with fusible links.

### 223 **2.1 Thermo-mechanical response induced by polymer phase separation.**

224 Phase transition in polymers plays a central role not only in the scientific understanding of  
225 condensed matter but also in their technological development.<sup>49</sup> In macromolecular

226 solutions or for swollen polymer networks, the solubility, and swelling properties,  
227 respectively, strongly depend on the polymer/solvent interactions. For a given binary  
228 system, polymer/solvent, these interactions vary with temperature and these variations can  
229 lead in certain cases to a continuous or discontinuous phase transition around a critical  
230 temperature.<sup>59</sup> Crossing the phase transition temperature ( $T_c$ ), polymer solutions as well as  
231 covalent hydrogels experience a tremendous change in viscoelastic properties. Based on  
232 the change of their solubility with temperature, thermo-responsive polymers can be  
233 classified into two opposite categories: polymers with a Lower Critical Solution  
234 Temperature (LCST) or an Upper Critical Solution Temperature (UCST).

#### 235 2.1.1 LCST-type thermo-responsive mechanical hydrogels

236 Although this is not really the phase transition temperature that can be predicted from the  
237 classical Flory-Huggins theory for polymer solutions, LCST is the most widely used  
238 thermal transition for polymer in aqueous media due to huge number of polymer/water  
239 systems that exhibit this behavior. The LCST is the critical temperature below which the  
240 components of the mixture are fully miscible for all compositions. Typically, the polymer  
241 chains, in the coil-state in water at low temperature, will collapse into a globular state above  
242 the transition temperature and aggregate to form a polymer-rich phase in equilibrium with  
243 a dilute polymer solution. Among the large amount of LCST polymers,<sup>60</sup> poly(*N*-  
244 isopropylacrylamide) (PNIPAm) is by far the most studied since the pioneering works on

245 the phase transition of gels in aqueous media.<sup>61</sup> Due to its chemical stability, low toxicity,  
246 low pH dependence,<sup>62</sup> electroneutrality, and its LCST ( $\sim 32^\circ\text{C}$ ) close to body temperature  
247 and easily adjustable with comonomers, PNIPAm hydrogels have been considered for  
248 many applications.

249 As a pioneering work, Takigawa et al.<sup>63</sup> demonstrated that Young's modulus of homo-  
250 PNIPAm hydrogel was increased by more than one decade upon heating above  $T_c$ . During  
251 phase separation, the PNIPAm chains self-associate and form a rich-polymer percolating  
252 framework which serves as a load-bearing phase to increase gel stiffness, extensibility, and  
253 toughness by enhancing energy dissipation (Figure 3a). A linear stress-strain behavior was  
254 observed for PNIPAm hydrogel, both below and above the LCST, while later this linearity  
255 was observed only at small strains.<sup>64</sup> Thereafter, many efforts were devoted to the thermo-  
256 responsive toughening of PNIPAm hydrogels.<sup>65-67</sup> Recently, by incorporating monomers or  
257 other organic or inorganic compounds into the PNIPAm network (copolymers,<sup>68</sup>  
258 topological hydrogel<sup>69-71</sup> or nanocomposites<sup>72</sup>) the resulting soft materials have  
259 demonstrated thermo-toughening performance comparable to homo-PNIPAm hydrogels.  
260 In these cases, the transition temperature of hydrogels can be finely tuned with the  
261 incorporation of the other component, no matter chemically copolymerized in the PNIPAm  
262 network or physically mixed,<sup>73-74</sup> to meet the demand of specific applications. In this  
263 context, the mechanisms of volume-phase transition in polymer gels have been intensively  
264 discussed, both experimentally and theoretically, from the viewpoint of structure, dynamics,

265 kinetics, and equilibrium thermodynamics.<sup>75</sup> For more details, readers may refer to the  
266 recent review elsewhere.<sup>76</sup>

267 During micro-phase separation, the coil/globule transition undergone at the molecular level  
268 by the elastically active PNIPAm chains usually gives rise to a macroscopic shrinkage of  
269 the gels, termed as “volume phase transition”.<sup>50</sup> Although this feature can endow the  
270 materials with potential applications in specific fields such as sensors and actuators, it  
271 hinders many practical perspectives relative to mechanical properties. For example, it is  
272 sometimes unnecessary or even undesirable to have a soft material that swells or shrinks  
273 during use. In addition, the volume contraction that accompanies the phase separation  
274 complicates the interpretation of the exact role of the two-phase morphology on the  
275 mechanical properties. It is indeed difficult to separate the intricate contributions of the  
276 phase separation and the change in polymer concentration.<sup>50</sup>

277 To solve this puzzle, Guo et al. developed highly swollen networks with different  
278 topologies capable of undergoing phase separation with significant modification of their  
279 mechanical properties without any change of their macroscopic dimensions (phase  
280 transition in isochoric conditions). A first topology was designed by grafting hydrophilic  
281 poly(*N,N*-dimethylacrylamide) (PDMA) side chains on a thermo-responsive PNIPAm  
282 network (PNIPAm-*g*-PDMA gel or GPN-D) (Figure 3b). Above  $T_c$ , the thermo-responsive  
283 PNIPAm backbone phase separates and forms a concentrated load-bearing scaffold

284 accounting for less than 10% of the whole volume, while the swelling pressure of the  
285 hydrophilic PDMA side chains allows to maintain the high level of hydration of the gel  
286 avoiding any volume phase transition. As shown in Figure 3c, the gel effectively retains its  
287 original dimensions set by the preparation state on either side of  $T_c$ . Unlike conventional  
288 covalent bonds, the physical interactions between PNIPAm backbones triggered by the  
289 phase separation process have low selectivity and can easily break and reform, ensuring  
290 topological adaptation of the stretched network as well as a greater ability to dissipate  
291 energy. From small-angle neutron scattering (SANS), it was shown that this gel gave rise  
292 to a bi-continuous structure that aligned under loading at high temperature. By comparison  
293 with the mechanical properties at low temperature, at high temperature the hydrogels  
294 achieved fracture stress and an elastic modulus 10 times higher and extensibility twice as  
295 large (Figure 3d). The deformation of the rich-PNIPAm phase also leads to significant  
296 dissipative processes and high toughness (fracture energy  $\sim 1000 \text{ J.m}^{-2}$ ). Interestingly, this  
297 was also the first time that an unusual crack bifurcation pattern has been reported in the  
298 field of hydrogels; such behavior having been observed mainly with natural rubbers (Figure  
299 3e).

300 During subsequent works, it was shown that the mechanical performances of these thermo-  
301 responsive hydrogels were strongly dependent on the architecture of the networks.<sup>77-79</sup> In  
302 particular, the length and density of hydrophilic grafts are crucial: shorter PDMA chains  
303 lead to much less pronounced fracture resistance, while higher graft density results in lower

304 fracture energy due to the lower fraction of PNIPAm domains (Figure 3f). By comparison,  
305 a hydrogel of opposite topology was prepared with the same PNIPAm/PDMA weight ratio  
306 (50/50) but this time by introducing PNIPAm grafts onto the crosslinked PDMA network  
307 (GPD-N gel). While exhibiting a similar phase separation process upon heating induced by  
308 PNIPAm side chains, this hydrogel showed much lower resistance to fracture than the  
309 previous GPN-D gel with no evidence of crack bifurcation.<sup>77</sup> From SANS experiments, a  
310 micellar architecture has been proposed with a swollen PDMA network physically  
311 crosslinked via PNIPAm aggregates. With this topology, the thermo-reinforcement  
312 increases with the size of PNIPAm sidechains, keeping constant the weight ratio  
313 PNIPAm/PDMA.<sup>79</sup> In fact, this strategy of reinforcement induced by a microphase  
314 separation process is somehow similar to that used in the case of nanocomposite gels where  
315 macromolecular chains are strongly anchored to the surface of inorganic particles.<sup>80</sup> The  
316 main difference, in the case of GPD-N gels, is that it is the chains of PNIPAm that self-  
317 associate to form their own reinforcement domains. In all cases, these organic or inorganic  
318 “fillers” act as additional crosslinkers increasing the elastic modulus but also the  
319 dissipation phenomena to pull off the chain either from the surface of the inorganic particle  
320 or from the polymer microdomain.

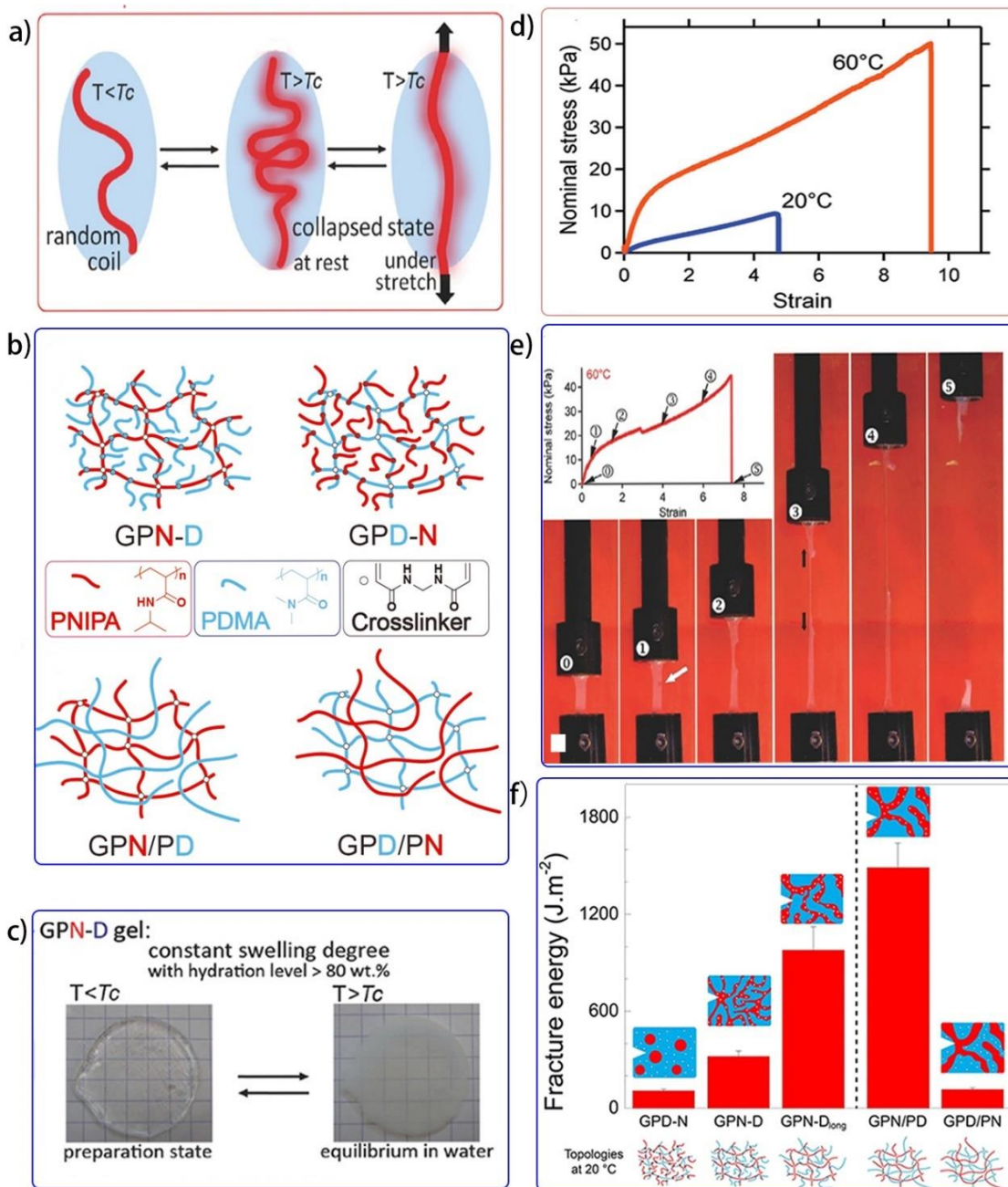
321 Compared to previous grafted architectures, other hydrogels such as semi-interpenetrated  
322 networks (semi-IPN) have also demonstrated similar thermo-responsive mechanical  
323 performance by forming comparable microstructure and giving rise to a similar mode of

324 crack propagation.<sup>78</sup> From a general point of view, the main characteristics of the thermo-  
325 reinforcement demonstrated with the grafted gels are reproduced with the semi-IPNs and  
326 the best properties are obtained with the semi-IPN prepared from a crosslinked PNIPAm  
327 network. It is therefore important to form during the phase separation a percolating network  
328 (here the crosslinked PNIPAm) as thick as possible which will play the key role of the load-  
329 bearing scaffold while keeping in mind that the hydrophilic counterpart remains important  
330 to preserve a high level of hydration at high temperature.

331 As the topology of hydrogels has a strong impact on thermo-responsive behavior, the  
332 precise construction of network structure is essential for the development of hydrogels with  
333 improved mechanical properties. Recently, Ida et al.<sup>81-85</sup> prepared a series of PNIPAm-  
334 based hydrogels by post-polymerization method, revealing that the type of copolymer  
335 network, the feed molar ratio, and the sequence of monomers effectively affected the  
336 hydrogel structure, the sharpness of the thermodynamic transition, and the mechanical  
337 properties. Well-designed amphiphilic structures with crosslinked PNIPAm domains were  
338 formed by post-crosslinking the end-blocks of triblock prepolymers with PNIPAm block  
339 either at the middle or at the ends. Compared to the hydrogels with a random sequence of  
340 monomers and crosslinkers with the same composition, Ida's hydrogels showed a faster  
341 and sharper volume phase transition upon temperature change as well as higher elastic  
342 modulus.<sup>81-82</sup> Thermally responsive crosslinked PNIPAm domains collapse when heated  
343 and they act as fillers by dissipating energy and improving hydrogel toughness as

344 previously described. Interestingly, the amphiphilic hydrogels designed with these thermo-  
345 responsive crosslinked domains can be studied under the preparation state while preserving  
346 isochoric conditions on either side of the phase transition temperature. Under these  
347 conditions, it is possible to specifically analyze the impact of the phase transition on the  
348 elastic modulus and the extensibility during heating.<sup>81</sup>

349 While hydrogels derived from PNIPAm have drawn considerable attention to thermo-  
350 responsive toughening performance, some weaknesses remain. One of the major  
351 drawbacks of these gels concerns their relatively weak mechanical properties, in particular  
352 their low elastic modulus ( $\sim$  a few tens of kPa) and fracture stress ( $< 100$  kPa) even above  
353 the transition temperature. Moreover, while the PNIPAm chain undergoes a relatively sharp  
354 coil/globule transition on a small temperature scale,<sup>86</sup> the corresponding hydrogels undergo  
355 a much smoother and gradual mechanical toughening, giving rise to a large hysteresis  
356 between heating and cooling processes. This kinetic behavior is closely dependent on the  
357 rate of temperature change. It is mainly due to the low collective diffusion coefficient of  
358 PNIPAm chains forming the 3D network, as well as to a strong slowing down of their  
359 mobility during the formation of very concentrated domains.<sup>74</sup> This is the case for example  
360 with the fracture energy of GPN-D hydrogels which increases from 100 to 1000 J.m<sup>-2</sup> over  
361 a wide temperature range from 33 to 60 °C.<sup>87</sup>



362

363 Figure 3. LCST-type thermo-responsive toughening of hydrogels. a) Schematic diagram  
 364 representing the conformation of PNIPAm at different temperatures. The collapsed PNIPAm  
 365 chains are defined as the load-bearing phase. Reproduced with permission.<sup>87</sup> Copyright 2016  
 366 WILEY-VCH Verlag GmbH & Co. KGaA, Weinheim. b) Schematic structure of thermo-  
 367 responsive graft hydrogels GPN-D, GPD-N, and semi-IPN hydrogels GPN/PD, GPD/PN.  
 368 Reproduced from<sup>78</sup> Copyright 2016 American Chemical Society. c) GPN-D gel is able to avoid

369 volume phase transition with relatively high hydration level (water content  $\cong$  83 wt%).  
370 Reproduced with permission.<sup>87</sup> Copyright 2016 WILEY-VCH Verlag GmbH & Co. KGaA,  
371 Weinheim. d) Uniaxial tensile stress-strain curves of GPN-D at 20 °C and 60 °C. e) Photos of GPN-  
372 D gels at 60 °C undergoing fracture test, which illustrate the crack bifurcation process.  
373 Reproduced with permission.<sup>87</sup> Copyright 2016 WILEY-VCH Verlag GmbH & Co. KGaA,  
374 Weinheim. f) Fracture energies obtained with PNIPA/PDMA hydrogels at 60 °C. Reproduced  
375 from<sup>78</sup> Copyright 2016 American Chemical Society.

376

377 Besides the thermo-responsive PNIPAm-based hydrogels which are by far the most studied,  
378 other LCST-type hydrogels have also demonstrated similar toughening behavior in  
379 response to the thermal trigger. Shibayama et al. have recently reported the synthesis and  
380 characterization of poly(oligo-ethylene glycol methyl ether methacrylate)-based gels  
381 prepared with two monomers having different ethylene oxide chain lengths ( $n = 2$  and  $n =$   
382  $4-5$ ).<sup>88</sup> By changing the comonomer ratio, they were able to change the LCST of the  
383 polymer network as well as the association process above the transition temperature  
384 providing a large spectrum of elastic to viscoelastic transitions with temperature. Although  
385 this study was carried out under isochoric conditions, giving rise to specific information on  
386 the biphasic morphology, the analysis of the mechanical properties was limited to small  
387 deformation. As reported with PNIPAm-based hydrogels,<sup>77</sup> the comparable shear modulus  
388 obtained at small strain and high temperatures could hide large differences in fracture  
389 energies (Figure 3f). Therefore, it seems important to systematically extend the analysis to  
390 large deformations to deepen the mechanical characteristics of gels and in particular the

391 impact of dissipative processes on fracture phenomena. Indeed, while the previous reported  
392 GPN-D hydrogel exhibits fracture energy 10 times higher than that of its GPD-N  
393 counterpart of the same composition at 60 °C, they exhibit similar elastic behavior when  
394 studied at small deformation.<sup>78</sup>

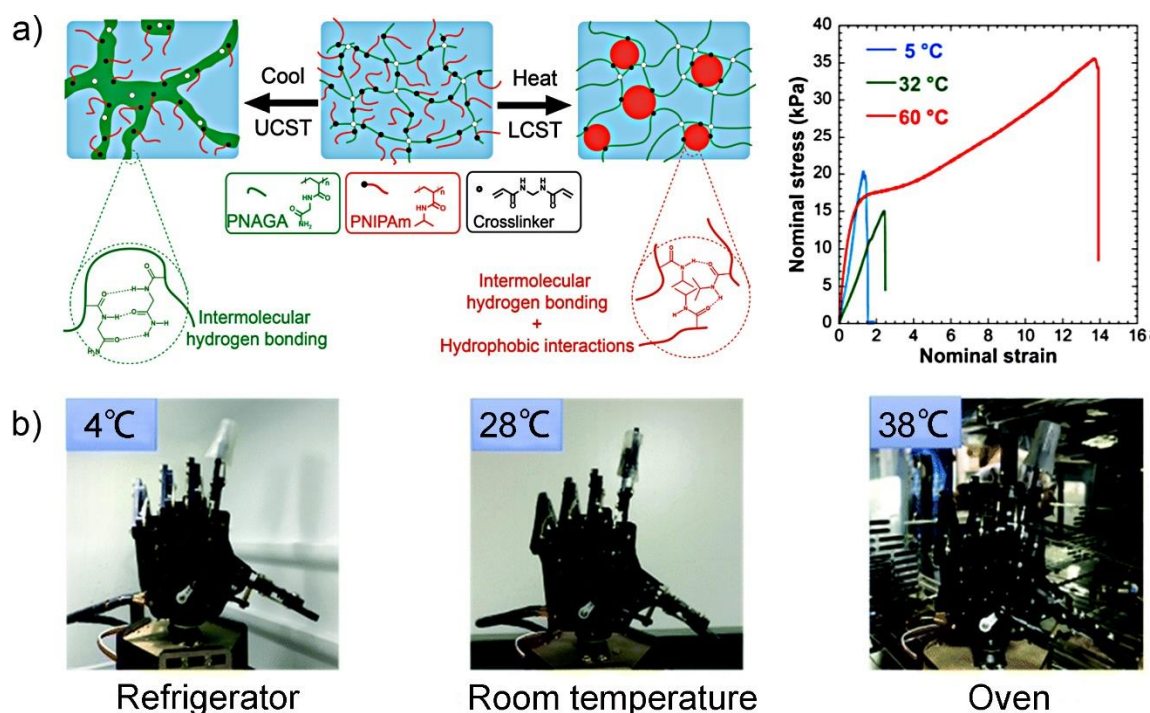
### 395 2.1.2 Thermo-responsive mechanical properties of UCST-type hydrogels

396 In contrast to LCST type hydrogels, thermo-responsive polymer networks with an upper  
397 critical solution temperature (UCST) can dissolve in solvents above the UCST and start to  
398 phase separate below the UCST. In theory, many polymers show a UCST in a given solvent  
399 due to complex temperature dependences of the interaction parameter.<sup>89</sup> The key is whether  
400 the thermo-triggered phase transition takes place under gentle conditions as expected for  
401 hydrogels (typically between 0-100 °C). UCST-type polymers, which are based on specific  
402 interactions (hydrogen bonding and/or electrostatic interactions), can be mechanically  
403 reinforced by cooling below  $T_c$  and weakened by heating above the transition temperature.  
404 Compared to LCST-type hydrogels, UCST ones remain much less explored mainly due to  
405 the few available polymer candidates.<sup>89-90</sup>

406 As a representative example of UCST-type polymers, poly(*N*-acryloylglycinamide)  
407 (PNAGA) was discovered over half a century ago and widely used in supramolecular  
408 chemistry.<sup>91</sup> Upon heating, highly concentrated PNAGA solutions demonstrate interesting  
409 mechanical performance with good stability and thermo-thinning properties.<sup>92</sup> Interestingly,

410 by anchoring LCST-type PNIPAm side-chains to a UCST network of PNAGA, Guo et al.<sup>93</sup>  
411 have developed new thermo-responsive hydrogels with double temperature response. By  
412 adjusting the composition between PNAGA and PNIPAm, it is possible to work in  
413 isochoric conditions while exploring the two independent phase transitions (UCST and  
414 LCST). As a result, the temperature range can be divided into three different domains: 1)  
415 low temperatures ( $T < UCST$  and  $LCST$ ), 2) intermediate temperatures ( $UCST < T <$   
416  $LCST$ ), and 3) high temperatures ( $T > UCST$  and  $LCST$ ). In the case of this dual thermo-  
417 responsive network, the mechanical modifications triggered by opposite phase transitions  
418 are dissimilar. At high temperature ( $T > UCST$  and  $LCST$ ), the PNIPAm side-chains  
419 collapse and self-associate into concentrated domains through hydrophobic interactions  
420 coupled with intra- and inter-molecular hydrogen bonds. These strong interactions give rise  
421 to the enhancement of both rigidity and extensibility as already described with hydrophilic  
422 PDMA network grafted with PNIPAm side-chains. By comparison, the phase separation of  
423 PNAGA at low temperature ( $T < UCST$  and  $LCST$ ) does not involve hydrophobic  
424 interactions and the intra- and inter-chain associations related to the formation of hydrogen  
425 bonds are weaker due to the stronger competition from water molecules for binding sites.  
426 The phase transition of the PNAGA network leads to an increase of the Young modulus,  
427 similar to that observed at high temperature with the phase transition of the PNIPAm chains,  
428 but to a strain at break 10 times lower (Figure 4a). This clearly underlines the importance  
429 of exploring the mechanical properties of gels at both small and large deformations. Indeed,

430 this feature may help to explain analogous phenomena reported with other UCST hydrogels,  
 431 including zwitterionic<sup>94</sup> or neutral<sup>95</sup> systems. In addition to changes in mechanical  
 432 properties, PNAGA-based dual thermally responsive hydrogels<sup>96</sup> also exhibit the obvious  
 433 transparency variation upon temperature disturbing, which makes it possible as an  
 434 electronic skin to qualitatively evaluate the ambient temperature (Figure 4b).



435

436 **Figure 4. UCST-type thermo-responsive toughening of hydrogels.** a) Schematic representation of  
 437 thermo-responsive self-assembly and mechanical properties of PAN (NAGA monomer and  
 438 PNIPAm) hydrogels upon temperature change. Figure colored for better illustration. Original in  
 439 black and white. Reproduced with permission.<sup>93</sup> Copyright 2017 WILEY-VCH Verlag GmbH &  
 440 Co. KGaA, Weinheim. b) Hydrogel as the robot's electronic skin to test different environment  
 441 temperatures (refrigerator, room temperature, and oven). Reproduced with permission.<sup>96</sup>  
 442 Copyright 2021 The Royal Society of Chemistry.

443

444 In addition to these synthetic systems, similar strategies have been developed on the basis  
445 of single or double networks by coupling covalent bonds with physical interactions  
446 involving bio-based molecules or polymers capable of self-associating by cooling. This is  
447 the case for example with low molecular weight gelators combining guanosine, borax, and  
448 potassium hydroxide which can form a supramolecular network within a covalent hydrogel  
449 of PDMA,<sup>97</sup> with crosslinked polyacrylamide networks interpenetrated with agarose chains  
450 which are known to reversibly form physical gels upon cooling<sup>98-99</sup> or with covalently  
451 cross-linked gelatin capable of forming additional physical junctions (triple helices) by  
452 cooling.<sup>100</sup> All these studies have demonstrated that the formation of second physical  
453 network results in a dramatic increase in strength and toughness at room temperature;  
454 physical interactions making an essential contribution to the dissipation process. In these  
455 cases, heating/cooling cycles have been mainly applied to promote mechanical recovery  
456 after large deformations and self-healing properties rather than studying the variation in  
457 mechanical properties throughout the thermal transition.

## 458 2.2 Thermo-responsive mechanical properties of hydrogels with glassy-like transitions

459 While thermo-softening hydrogels involving UCST polymers remain relatively rare,  
460 thermo-softening materials are ubiquitous in nature. In the field of the polymer industry,  
461 for instance, thermo-softening plastics, more usually termed thermoplastics, are widely

462 used for manufacturing a wide variety of items as they are easily pliable or moldable above  
463 their softening temperature and solidifies upon cooling. At the molecular level, the polymer  
464 segments initially in the frozen state acquire mobility when the temperature is raised above  
465 the glass transition temperature ( $T_g$ ), switching the polymer materials from the rigid glassy  
466 state to the soft rubbery state.<sup>101</sup> Without a doubt, this feature is not exclusive to non-solvent  
467 materials: a global group of researchers has attempted to apply this strategy in the  
468 preparation of thermo-softening hydrogels.

469 In recent years, Wu's group has designed a series of robust hydrogels following this  
470 strategy. As a typical example, ultra-stiff and tough hydrogels have been prepared by  
471 copolymerizing methacrylic acid (MAAc) and methacrylamide (MAAm) in water.<sup>102</sup>  
472 Indeed, the strong interactions between acid and amide groups allow the formation of a  
473 dense and robust hydrogen bond network which gives the material temperature-dependent  
474 mechanical properties. Below the transition temperature ( $T_c$ ), hydrogels display  
475 considerable stiffness due to the glassy behavior of the polymer phase, with a tensile stress  
476 of 4-11 MPa and strain of 400-600%. The sharp decrease in tensile stress detected above  
477  $T_c$  gives these materials mechanical shape memory properties (Figure 5a). Later, the  
478 structure-properties relationships and the kinetics of the structure formation have been  
479 further investigated to reveal the mechanism of thermo-responsive toughening.<sup>103</sup>  
480 Moreover, systematic researches involving dynamic hydrogen bonds have been carried  
481 out to illustrate the concept of glass transition hydrogels as well.<sup>93, 94</sup>

482 More generally, hydrogels with similar thermo-softening performance have been reported  
483 in other systems with various noncovalent interactions, such as hydrogen bonds,<sup>104</sup>  
484 hydrophobic interactions,<sup>105-106</sup> and ionic bonds.<sup>107-109</sup> For example, Wang<sup>104</sup> has reported  
485 thermo-responsive poly(vinylpyrrolidone-*co*-acryloxy acetophenone) glassy hydrogels  
486 with high tensile strength (8.4 MPa) and Young's modulus (94 MPa) at room temperature.  
487 When heated to 90 °C, the elastic modulus of gels decreased over more than 3 decades  
488 making this rigid hydrogel a suitable candidate as a shape memory material for surgical  
489 fixation devices to wrap around and support various shapes of limbs. In another study,  
490 hydrogen bonds, dipole-dipole, and hydrophobic interactions were coupled by  
491 copolymerizing acrylonitrile with N-acryloyl-2-glycine. These tough hydrogels clearly  
492 demonstrate thermo-softening performance when heated from 10 °C (Young's modulus 430  
493 MPa) to 37 °C (Young's modulus 16 MPa). Due to the presence of carboxylic groups in  
494 the copolymer network, these hydrogels exhibit a shape memory responsive behavior,  
495 controllable by both temperature and pH, preparing them as attractive candidates for  
496 permanent embolic agents.<sup>110</sup>

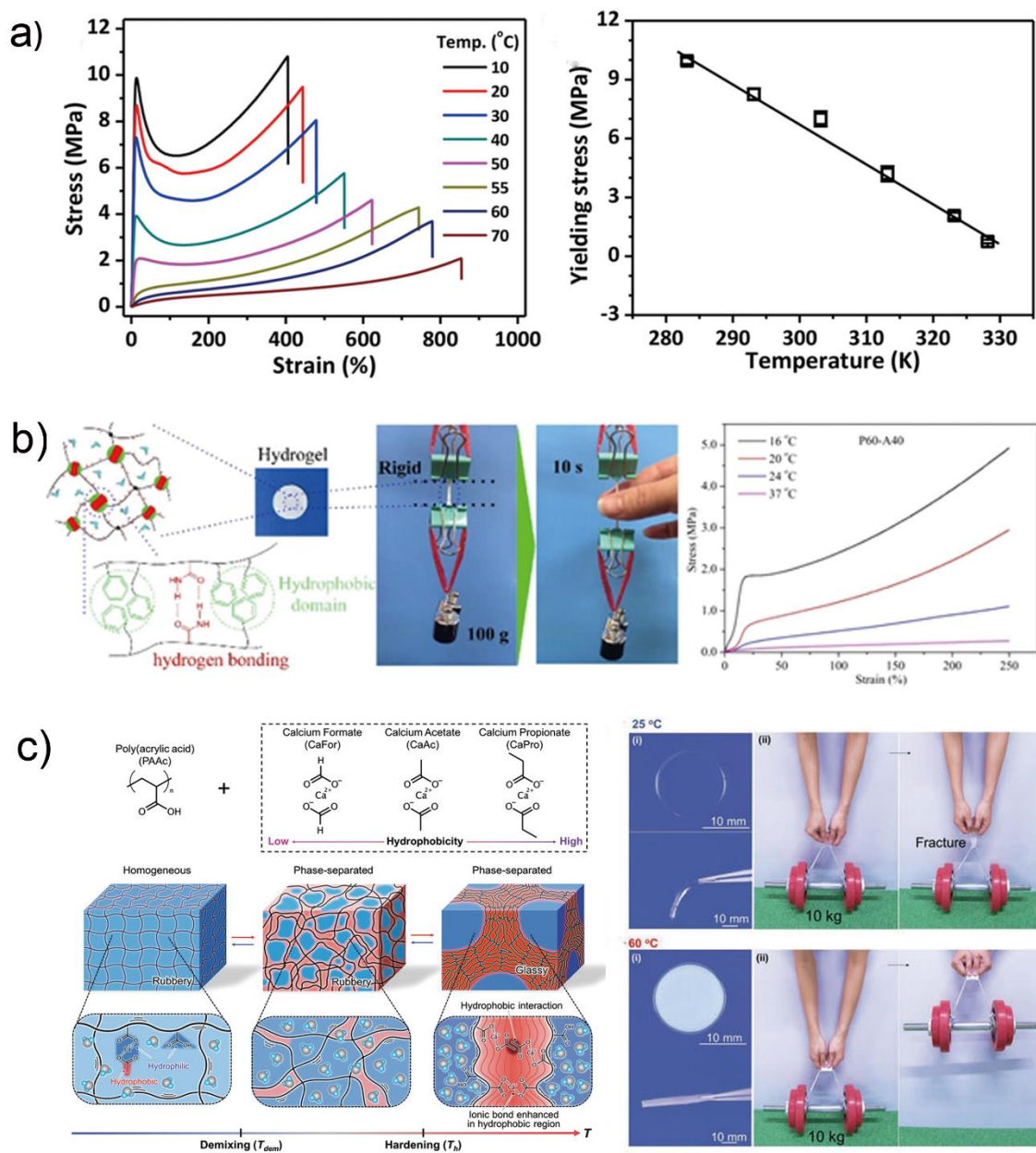
497 While most of this work of hydrogels associates the temperature dependence of mechanical  
498 properties with the existence of a glass transition, as judged by the softening performance,  
499 it is still unclear whether this transition is really of the same nature as that reported with  
500 thermoplastics. For instance, the relaxation times under  $T_g$  in conventional thermoplastics  
501 are essentially much longer than the typical duration of an experiment or a numerical

502 simulation,<sup>111</sup> while for some of these so-called “glassy hydrogels” the relaxation time is  
503 fairly short (e.g.  $\sim 1 \text{ s}^{102}$ ). Theoretically, hydrogels with glass transition behavior should  
504 generally be designed with high  $T_g$  hydrophobic polymers. However, scientists can  
505 effectively prepare tough hydrogels with rather low glass transition polymer networks,  
506 which also demonstrate a glassy-like transition. As a typical example, Liang et al.<sup>112</sup>  
507 ingeniously designed a body temperature-responsive hydrogel based on the  
508 copolymerization of hydrophobic 2-phenoxyethyl acrylate (PEA,  $T_g$  of polymer  $\sim 16 \text{ }^\circ\text{C}$ )  
509 and hydrophilic acrylamide. Within these hydrogels, the high fraction of hydrophobic  
510 monomers is responsible for the low content of water at equilibrium (less than 50 wt%), as  
511 the aggregation of PEA moieties provides a hydrophobic micro-environment for the  
512 adjacent amide groups which further stabilize their intermolecular hydrogen bonds. The  
513 scission of dynamic hydrogen bonds between acrylamide units by increasing the  
514 temperature is then responsible for the thermo-responsive performance. As shown in Figure  
515 5b, the hydrogel exhibits very high tensile strength at low temperature along with a high  
516 yield stress and good extensibility, highlighting high energy dissipation. These mechanical  
517 properties are highly temperature-dependent: just after heating by hand for a few seconds,  
518 the hydrogel becomes weak without any distinct signature of yielding.

519 Similar to thermoplastics which weakens above  $T_g$ , all of the aforementioned hydrogels  
520 demonstrate thermo-softening performance, which precludes their use in applications  
521 which require high mechanical properties at elevated temperature. Although hydrogels

522 designed with LCST-type polymers are good candidates for improving mechanical  
523 properties by heating, the phase separation kinetics, as well as moderate mechanical  
524 performances, requires the system to be further improved. Recently, inspired by the  
525 molecular mechanism of thermally stable proteins, Gong et al.<sup>30</sup> developed a novel thermo-  
526 responsive hydrogel that undergoes ultra-rapid, isochoric, and reversible switching from  
527 soft hydrogels to rigid plastic-like material with increasing temperature. The materials were  
528 prepared from inexpensive and non-toxic poly(acrylic acid) (PAAc) hydrogels containing  
529 calcium acetate. The synergistic combination of hydrophobic and ionic interactions leads  
530 to phase separation by heating with a subsequent rubbery-to-glassy transition at higher  
531 temperature. Crossing the transition temperature, the material's stiffness, strength and  
532 toughness increased 1800-, 80-, and 20-folds, respectively, and a thin gel sheet could  
533 support a 10 kg weight (Figure 5c). This work may significantly broaden the scope of  
534 thermally stiffened polymer applications, such as for heat absorption or in protective  
535 sportswear.

536



537

538 **Figure 5. Thermo-responsive hydrogels based on the glassy-like transition. a) Tensile stress-strain**  
 539 **curves and yielding stress of poly(methacrylamide-*co*-methacrylic acid) (P(MAAm-*co*-MAAc))**  
 540 **gel at different temperatures. Reproduced from<sup>102</sup> Copyright 2019 American Chemical Society. b)**  
 541 **Photo illustration of body temperature-dependent mechanical strength and uniaxial tensile**  
 542 **behavior of a poly(2-phenoxyethyl methacrylate-*co*-acrylamide) (P(PEA-*co*-AAM)) hydrogel with**  
 543 **60 mol% of PEA and 40 mol% of AAm (P60-A40). The sheet was rigid at a surrounding**

544 **temperature of 10 °C and could bear a 100 g weight without any obvious deformation. However,**  
545 **upon heating by two fingers, the hydrogel became soft and was gradually stretched by the loaded**  
546 **weight. Reproduced from<sup>112</sup> Copyright 2019 American Chemical Society. c) Mechanism of**  
547 **thermo-induced instant switching from soft hydrogel to hard plastic-like materials by**  
548 **polymerizing PAAc hydrogel in presence of calcium ions. Pictures show a load of materials at low**  
549 **and high temperatures, where the gels become significantly toughened up with increasing**  
550 **temperature. Reproduced with permission.<sup>30</sup> Copyright 2020 Wiley-VCH Verlag GmbH & Co.**  
551 **KGaA.**

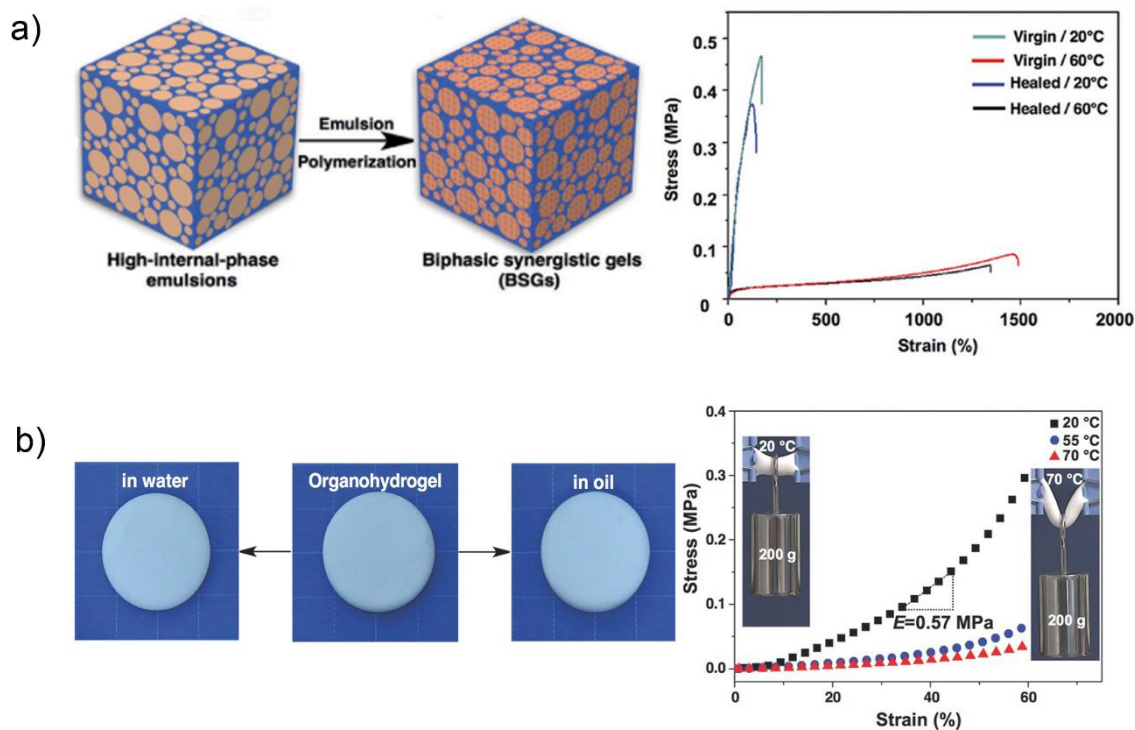
552

### 553 2.3 Thermo-responsive mechanical properties of hydrogels with fusible links

554 As we know, crystalline materials are significantly softened by heating above their melting  
555 point. This first order thermodynamic transition has also been used to develop thermo-  
556 responsive hydrogels by introducing fusible links in the macromolecular architecture. In  
557 this context, several strategies have been considered: either from semi-crystalline networks  
558 or by adding crystalline additives.

559 A typical example of such hydrogels was prepared by copolymerization of crystallizable  
560 n-stearyl acrylate (SA) segments into a hydrophilic poly(acrylic acid) network. The  
561 mechanical properties of these materials exhibit a sharp temperature dependence when the  
562 temperature is raised above 50 °C with Young's modulus of hydrogels decreasing abruptly  
563 by about two orders of magnitude from  $10^7$  to  $10^5$  Pa.<sup>113</sup> Based on Small-Angle X-ray  
564 Diffraction and Differential Scanning Calorimetry experiments, it was shown that the long

565 stearyl side-chains, which self-organize at room temperature into crystalline lamellae  
566 aligned perpendicular to the main chain, undergo an order-disorder transition above 50 °C.  
567 The melting of these lamellae is then the driving force of the macroscopic transition which  
568 allows going from hard plastic to a soft and flexible material.<sup>114</sup> Similar thermo-responsive  
569 gels were prepared by Okay et al. through copolymerizing acrylic acid with 20-50 mol %  
570 of crystallizable n-octadecylacrylate.<sup>115</sup> In the network, hydrophilic segments provide  
571 flexibility to the network while hydrophobic units pack to form crystalline domains that  
572 render the material mechanically robust. These melt-processable hydrogels display very  
573 high compressive strength (90 MPa) and Young's modulus (26 GPa) as well as shape  
574 memory behavior and self-healing properties as expected for such associating systems. In  
575 further work, it revealed that the mechanical performance of these semi-crystalline thermo-  
576 responsive hydrogels is related to synthesis parameters, including the type<sup>116-117</sup> and the  
577 amount of the monomers,<sup>118</sup> the methods of polymerization,<sup>119</sup> the water content of the  
578 hydrogels<sup>120</sup>, and the amount of surfactant.<sup>115, 121</sup>



579

580 **Figure 6. Thermo-responsive hydrogels based with fusible links. a) Scheme and tensile stress-**  
 581 **strain curves of virgin and healed biphasic synergistic gels (BSGs) at 20 °C and 60 °C. Reproduced**  
 582 **with permission.<sup>122</sup> Copyright 2017 Wiley-VCH Verlag GmbH & Co. KGaA, Weinheim. b) Photos**  
 583 **of organohydrogels that exhibit nonswelling behavior in water or oil, and tensile stress-strain**  
 584 **curves of organohydrogel at 20 °C, 55 °C, and 70 °C. Reproduced with permission.<sup>123</sup> Copyright**  
 585 **2017 WILEY-VCH Verlag GmbH & Co. KGaA, Weinheim.**

586

587 However, these strategies for preparing thermo-switchable mechanical hydrogels depend  
 588 on relatively sophisticated molecular design and chemical modification. Although the  
 589 properties of these hydrogels are rather promising, their method of preparation is far from  
 590 optimal because it requires several steps with the synthesis in organic solvents, or in water  
 591 using a large amount of surfactant, followed by a purification step in pure water to obtain

592 the hydrogels. To overcome this problem, Zhao and coworkers<sup>122</sup> developed a one-pot  
593 strategy to synthesize biphasic synergistic gels, called organohydrogels, by in situ  
594 polymerization of oil-in-water high internal-phase emulsions; the oleophilic stearyl  
595 methacrylate acting as the oil phase (Figure 6a). The semi-crystalline behavior of closely  
596 packed micro-inclusions within the elastic hydrogel matrix not only greatly improves the  
597 mechanical properties of hydrogels, but also endows these materials with switchable  
598 mechanical behavior. As a result, these gels exhibit a broad spectrum of mechanical  
599 performance under tensile tests ranging from high modulus and low strain at break at 20 °C  
600 to low modulus and high strain at 60 °C. In further work, Liu et al.<sup>123</sup> applied this strategy  
601 using lauryl methacrylate as the oily phase, to prepare organohydrogels combining both  
602 high strain and tough shape memory properties. These biphasic materials can maintain  
603 isochoric conditions, both in water and in oil, and withstanding high load at different  
604 temperatures (Figure 6b).<sup>123</sup> During shape memory experiments, the material was shown  
605 to exhibit a high deformation capacity with fully recoverable deformation, both under  
606 stretch (up to 2600%) and under compression (up to 85%) by applying a load almost 20  
607 times greater than the weight of the material. In subsequent studies, the introduction of  
608 supramolecular interactions (e.g., acrylic acid/Fe<sup>3+</sup>) in the hydrophilic phase showed that  
609 it was possible to prepare organohydrogels responding to two orthogonal stimuli: the  
610 temperature for the crystalline oily phase and addition of a competitor for the  
611 supramolecular interactions.<sup>124</sup>

612

### 613 **3. Photo-responsive hydrogels**

614 Like temperature, light is another noninvasive trigger that allows remote, easy, and rapid  
615 manipulation of materials without the need of additional reagents, and therefore with  
616 limited byproducts.<sup>125</sup> Typically, the photo-responsiveness of hydrogels can be induced  
617 either by the 3D polymer network itself or by inorganic additives incorporated therein.  
618 While in the first case the photo-response generally leads to a variation in the degree of  
619 crosslinking by photoreaction, the use of additives more generally involves an overall  
620 photothermal response without variation in the degree of crosslinking.

#### 621 3.1 Light-responsive polymer networks

622 Typical photoreactions of polymers include cleavage,<sup>40</sup> addition,<sup>41</sup> exchange,<sup>42</sup> and  
623 isomerization.<sup>44-45</sup> *O*-nitrobenzyl ester is a typical example of cleavage-type functional  
624 groups that are currently used for the design of photo-responsive hydrogels.<sup>125</sup> For instance,  
625 the photo-labile bond of the 2-nitrobenzyl functional group of the hydrophobic monomer  
626 (2-nitrobenzyloxycarbonylaminoethyl methacrylate (NBOC)), can be irreversibly split  
627 under UV irradiation with the formation of hydrophilic 2-aminoethyl methacrylate (AMA)  
628 and the release of 2-nitrobenzaldehyde and CO<sub>2</sub>.<sup>126</sup> Starting from a linear copolymer of  
629 hydrophilic 2-ureidoethyl methacrylate (UM) and NBOC, poly(UM-*co*-NBOC), which

630 initially self-assembles through hydrophobic interactions between NBOC units, UV  
631 irradiation will cause a succession of chemical and physical events as follows 1) the  
632 transformation of hydrophobic NBOC groups into hydrophilic AMA units, 2) the  
633 disassembly of hydrophobic crosslinks and 3) the chemical reaction between amino groups  
634 of AMA and ester bonds of UM thus forming new chemical crosslinks.<sup>126</sup> As shown in  
635 Figure 7a, poly(UM-co-NBOC) hydrogels after UV irradiation exhibit a higher Young's  
636 modulus but lower failure strain and stress compared with those without UV irradiation.  
637 Due to the limited penetration thickness of UV, the hydrogel demonstrates a sandwiched  
638 structure with two rigid outer layers and a soft inner layer after UV irradiation. Under  
639 deformation, the outer layers fractured preferentially (like the first highly crosslinked  
640 network of a double network gel), while the inner layer maintained the whole integrity of  
641 hydrogels, playing a role resembling the second loosely crosslinked network of DN gels.  
642 By adjusting UV curing time and/or UV penetration length, the precise control of the  
643 sandwich structure can be finely achieved. The thinner the soft middle layer, the weaker  
644 the ability to bear the stretching and maintain global integrity.

645 Another elegant approach is to prepare hydrogels with photo-tunable crosslinking degrees  
646 via photo-addition reactions. Coumarin (COU), one of the well-known light-sensitive  
647 molecules, undergoes a [2+2] photo dimerization under irradiation at 365 nm while the  
648 resulting adduct can be decoupled by irradiation at 254 nm.<sup>127</sup> Sun et al.<sup>41</sup> have first  
649 prepared linear polyacrylamides bearing pendant COU groups. In the presence of  $\gamma$ -

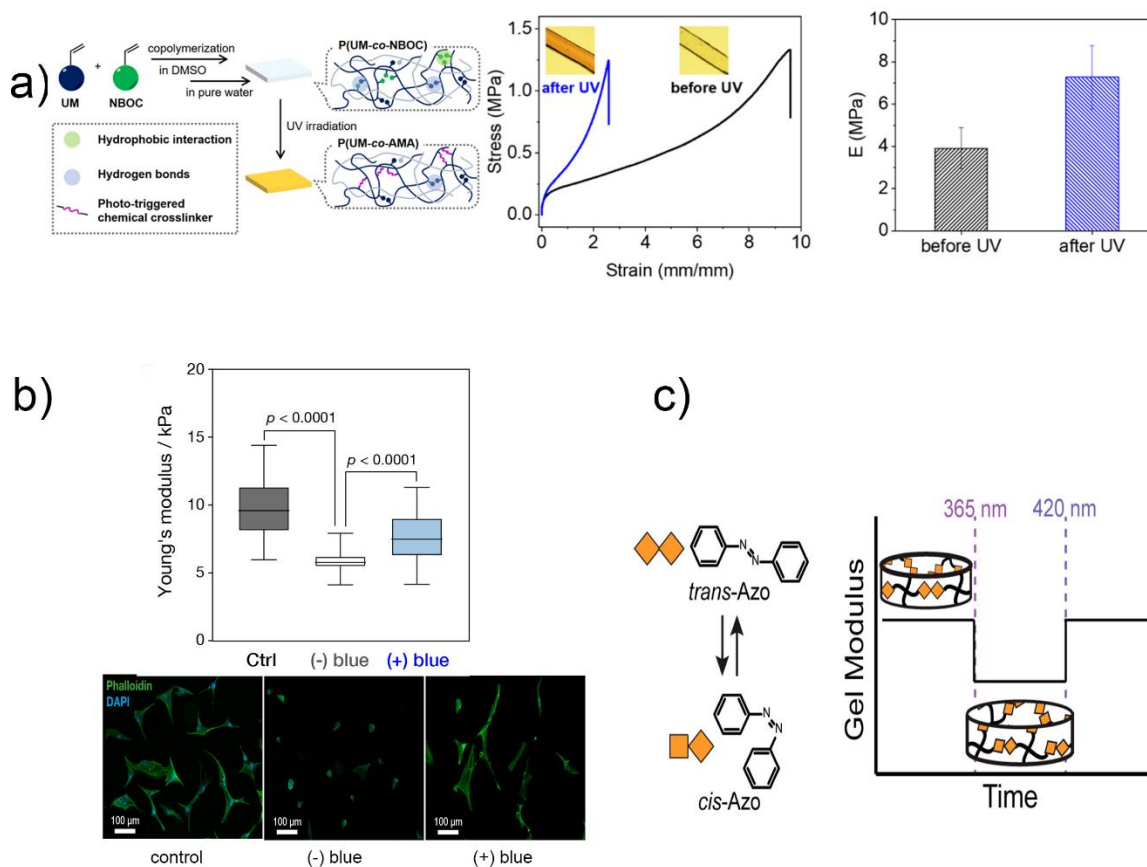
650 cyclodextrin ( $\gamma$ CD), which can host two molecules of COU, the initial polymer solution  
651 was transformed into a transient network with the formation of dynamic COU- $\gamma$ CD-COU  
652 interchain bonds. After irradiation at 365 nm, the dimerization of the 2 COU molecules  
653 hosted in the same  $\gamma$ CD cavity transforms the physical bond into a covalent bond which  
654 results in stiffening of the network with a doubling of the storage modulus. In contrast,  
655 when irradiated at 254 nm light, the chemical hydrogel turns back to a soft host-guest  
656 physical network.

657 In contrast to photo-responsive toughening of hydrogels via the tuning of covalent bonds,  
658 the possibility of using dynamic photo-reversible noncovalent interactions has been much  
659 less investigated. Very recently, it has been reported that photo-sensitive coordinate bonds  
660 can efficiently release the energy stored by the hydrogel.<sup>128</sup> The authors took  
661 poly(acrylamide-co-acrylic acid) (P(AAm-co-AAc)) hydrogel for illustration. After being  
662 prestretched and immersed in  $\text{Fe}^{3+}$  solution, the deformation of hydrogel is fixed by the  
663 coordinate bonds between  $\text{Fe}^{3+}$  and carboxyl groups from AAc units which temporarily  
664 store potential energy in hydrogels. After UV irradiation,  $\text{Fe}^{3+}$  is reduced to  $\text{Fe}^{2+}$ , resulting  
665 in the breakdown of the coordinate bonds and the fast release of the elastic potential energy  
666 stored in the hydrogel.<sup>128</sup> This strategy of storing and releasing elastic energy, based on the  
667 destabilization of the coordination bonds by photoreduction, endows hydrogels with an  
668 elasticity-plasticity switchability, multi-stable deformability in fully reversible and  
669 programmable manners, and anisotropic or isotropic deformations. With the high power

670 density and programmability via this customizable modular design, these hydrogels  
671 demonstrated potential for broad applications in artificial muscles, contractile wound  
672 dressing, and high-power actuators. In the same manner, photo-responsive adhesion can be  
673 easily achieved by tuning coordination bonds between  $\text{Fe}^{3+}$  and carboxyl groups.<sup>129</sup> Upon  
674 irradiation, the dissociation of complexes causes a strong decrease in the adhesion energy  
675 from 200 to 10  $\text{J m}^{-2}$ .

676 However, the above photo-cleavage and addition reactions are generally not fully  
677 reversible, which in some cases may limit the practical use of such materials.  
678 Comparatively, the use of photo-isomerization reactions makes it possible to prepare  
679 materials with satisfactory reversibility of their mechanical properties. Azobenzene, as a  
680 photo-responsive molecule, undergoes trans-to-cis and cis-to-trans isomerizations upon  
681 exposure to UV and blue light, respectively, resulting in a change of distance between the  
682 two phenyl rings (from 9 Å to 5.5 Å) and dipole moments (from 0.5 D to 3.1 D) for trans  
683 and cis isomers respectively. Hydrogels that incorporate photo-switchable molecules can  
684 exhibit reversible variations in stiffness as a function of the irradiation wavelengths. These  
685 stimuli-sensitive hydrogels are candidates to direct or probe osteogenic and myogenic  
686 differentiation of human mesenchymal stem cells (MSCs).<sup>130-131</sup> It has been reported that  
687 MSCs grown on substrates with varying stiffness express implicit changes, such as  
688 development, aging, and fibrosis. Upon blue light (490 nm), the polyacrylamide hydrogel  
689 containing 4,4'-diacrylamidoazobenzene becomes stiffer as the predominant trans isomer,

690 which is less polar, has a greater ability to self-associate. At the same time, cells exhibit a  
 691 better spreading with larger spread cell areas in these stiffer hydrogel substrates compared  
 692 to softer ones (Figure 7b).<sup>132</sup> In a similar work, a peptide crosslinker containing azobenzene  
 693 is introduced into poly(ethylene glycol) to form a light-responsive hydrogel. Upon  
 694 irradiation with cytocompatible doses of 365 nm light (UV), isomerization to the  
 695 azobenzene cis configuration leads to a softening of the hydrogel up to 100 – 200 Pa (shear  
 696 storage modulus). The modulus of the gel can be well tuned upon irradiation with light  
 697 with different wavelengths (Figure 7c). The planar trans conformation can better stabilize  
 698 the hydrogen bonds between the peptide cross-linkers and harden the substrate.<sup>133</sup>



699

700 **Figure 7. Photo-responsive hydrogels with tunable mechanics. a) Schematic illustration**  
701 **“sandwich” structured hydrogels composed of poly(2-ureidoethyl methacrylate-co-2-**  
702 **nitrobenzyloxycarbonylaminoethyl methacrylate) (P(UM-co-NBOC)) (yellow part) and poly(2-**  
703 **ureidoethyl methacrylate-co-2-aminoethyl methacrylate) (P(UM-co-AMA)) (gray part) hydrogels.**  
704 **Tensile stress-strain curves and corresponding Young’s modulus (E) of the hydrogels before and**  
705 **after UV irradiation are shown on the right. The inset images are cross-sectional micrographs of**  
706 **the sample. Reproduced from<sup>126</sup>. Copyright 2019 American Chemical Society. b) Young’s modulus**  
707 **of hydrogel after treatment and fluorescence microscopy images of mesenchymal stem cells**  
708 **(MSCs). Control gels (ctrl) that had not been exposed to UV. Blue gels were softened by exposure**  
709 **to UV (365 nm) irradiation for 30 min; (+) blue gels were exposed to blue (490 nm) light for 1 h,**  
710 **whereas (–) blue gels were unirradiated (left in the dark). Ctrl cells to be well spread, (–) blue cells**  
711 **to be smaller, and (+) blue cells to have recovered spreading. Reproduced from<sup>132</sup>. Copyright 2018**  
712 **American Chemical Society. c) Isomerization of azobenzene (Azo) group and modulus of gels upon**  
713 **light. Reproduced from<sup>133</sup>. Copyright 2015 American Chemical Society.**

714

### 715 3.2 Light-responsive additives

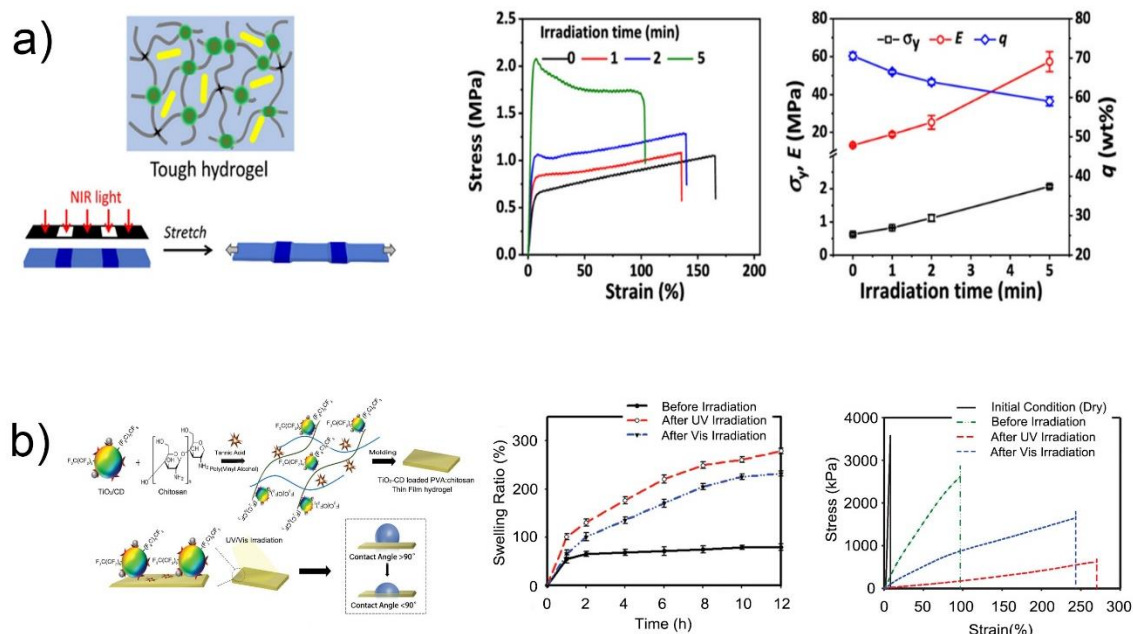
716 Along with the hydrogels described previously, in which the photosensitive molecules  
717 belong to the architecture of the polymer network, photo-stimulation properties can also be  
718 generated using thermo-responsive polymers and photo-sensitive inorganic fillers. Among  
719 the systems investigated, near-infrared (NIR) often serves as a light trigger while gold  
720 nanoparticles or nanorods,<sup>134-135</sup> ferrosferric oxide nanoparticles ( $\text{Fe}_3\text{O}_4$  NPs),<sup>136</sup> and  
721 graphene oxide (GO)<sup>137</sup> are generally used as photo-convertor. In response to irradiation,  
722 part of the light energy is converted into thermal energy, which is referred to as the

723 photothermal effect. As an example, Huang and co-authors<sup>138</sup> developed light- and thermo-  
724 responsive hydrogels by dispersing GO into interpenetrating networks formed by  
725 physically cross-linked gelatin and chemically cross-linked polyacrylamide. Without light  
726 irradiation, relatively high mechanical toughness (strength > 400 kPa and fracture strain >  
727 500 %) was achieved by the double-network which dissipates energy through the sacrificial  
728 gelatin network and GO particles bridging the two networks through supramolecular  
729 interactions. Under the NIR trigger, temperature increases rapidly and causes the  
730 dissociation of the thermo-responsive gelatin network which greatly declines the modulus  
731 of the gel. With optimal content of GO and enough NIR time, hybrid GO-based hydrogels  
732 display thermo-patterning and NIR irradiation erasing performances.

733 In another representative example, Wu and co-workers have developed stiff and tough  
734 shape memory hydrogels responding to NIR light irradiation by incorporating gold  
735 nanorods into a glassy gel matrix of poly(1-vinylimidazole-*co*-methacrylic acid)  
736 hydrogels.<sup>139</sup> Owing to the photothermal properties of gold nanorods, the localized  
737 temperature rise induced by the NIR light irradiation, which turns the hydrogel from rigid  
738 to soft by crossing the  $T_g$ .<sup>140</sup> After irradiation and cooling to room temperature, the  
739 hydrogels show an increase in Young's modulus ( $E$ ), from 13 to 57 MPa, and yielding  
740 stress ( $\sigma_y$ ), from 0.6 to 2.1 MPa, whereas the water content decreases from 71 to 59 wt%  
741 (Figure 8a). This behavior is attributed to the collapse of copolymer chains at high  
742 temperature (above  $T_g$ ) which leads to the formation of a denser network of hydrogen bonds

743 during cooling

744 The use of inorganic composite under light irradiation also proves to be an effective way  
745 to tune the hydrophilic/hydrophobic balance of the material and consequently adjust the  
746 mechanical properties of hydrogels. Recently, a sophisticated formulation of hybrid  
747 materials was developed by Park and co-workers via loading in a poly(vinyl  
748 alcohol)/chitosan matrix photocatalytic TiO<sub>2</sub>/CD particles (CD for silica-carbon dots)  
749 which exhibit a unique light absorption behavior with a wide UV-vis range of absorption  
750 wavelengths. In that system, metal oxides TiO<sub>2</sub> produces a photoelectric effect under UV  
751 activation, while the CDs demonstrate photoelectric properties due to the recombination of  
752 photo-excited electron-hole pairs. Under UV or visible irradiation, the photocatalytic  
753 nanomaterial changes the surface wettability of the thin-film hydrogel from hydrophobic  
754 to hydrophilic due to reactive oxygen (O<sup>2-</sup>) and hydroxide species (-OH) which were  
755 formed during the process. This hydrophilicity modification remarkably affects the  
756 permeability to water which swells the hydrogel and therefore modifies its mechanical  
757 behavior as well as its electronic properties (Figure 8b).



758

759 **Figure 8. Photo-responsive hydrogels with tunable mechanics induced by embedded additives. a)**  
 760 **Schematic and light responsive performance of poly(1-vinylimidazole-*co*-methacrylic acid)**  
 761 **hydrogels integrated with 3 nM of gold nanorods. The tensile stress-strain curves and the**  
 762 **corresponding Young's modulus ( $E$ ) and yielding stress ( $\sigma_y$ ), as well as the water content ( $q$ )**  
 763 **determined as a function of irradiation time are shown on the right. Reproduced from<sup>139</sup>.**  
 764 **Copyright 2020 American Chemical Society. b) Scheme of the hydrogel thin-film based on**  
 765 **titanium oxide (TiO<sub>2</sub>) polydopamine-perfluorosilica carbon dot (CD)-conjugated chitosan-**  
 766 **polyvinyl alcohol-loaded tannic acid along with UV and vis irradiation response affecting the**  
 767 **surface hydrophilicity. The force-displacement curve and the swelling ratio of the hydrogel are**  
 768 **shown on the right. Reproduced with permission.<sup>141</sup> Copyright 2019 WILEY-VCH Verlag GmbH**  
 769 **& Co. KGaA, Weinheim.**

770

771 Although sharing various comparable advantages to the temperature stimulus, the light  
 772 trigger is much less utilized, mainly due to the intrinsic feature of light. On one hand, upon

773 irradiation with relatively short-wave light such as UV, the short penetration depth is often  
774 a critical shortcoming.<sup>142</sup> In certain cases, the high density also led to the degradation of  
775 the network's backbone.<sup>143</sup> On the other hand, relatively long-wave light such as NIR is  
776 often unable to provide enough energy to initiate photoreactions.

#### 777 **4. pH-sensitive hydrogels**

778 pH-responsive hydrogels are a subset of stimuli-responsive systems capable of responding  
779 to pH environment. Weak polyelectrolyte hydrogels containing partially ionizable acidic  
780 units such as acrylic acid or methacrylic acid will become negatively charged with  
781 increasing the pH, typically above their pKa, and their counter-ions induce a huge increase  
782 of the osmotic pressure. On the other hand, hydrogels containing weak basic groups, like  
783 dimethylaminoethyl acrylate or 1-vinylimidazole, become cationic by lowering the pH.<sup>144</sup>  
784 As acidic or alkaline conditions have a significant impact on the strength of physical  
785 interactions, such as hydrogen bonds or ligand-metal coordinate bonds, they can be used  
786 to tune the macroscopic properties of hydrogels. In addition, the responsive ionization of  
787 networks at different pH also leads to significant volume change with osmotic pressure.  
788 This will greatly influence the mechanical properties of the hydrogels but in the following  
789 examples the impact of the physical interactions on the elastic properties is much greater  
790 than that linked to the variation in volume as given by  $G \sim Q^{-b}$  with scaling exponent  $b =$   
791  $1/3$  in  $\theta$  conditions and  $b = 7/12$  in a good solvent.

## 792 4.1 Hydrogen bonds

793 A hydrogen bond is an electrostatic attraction between polar molecules that occurs when a  
794 hydrogen atom is bound to a highly electronegative atom such as nitrogen, oxygen, or  
795 fluorine.<sup>145</sup> These combinations are not stable enough, especially in aqueous media with  
796 pH disturbing. For instance, the deprotonation of -COOH in a basic environment leads to  
797 the breaking of the transient network of hydrogen bonds formed by the carboxylic  
798 groups.<sup>146-147</sup>

799 Zhang and co-authors reported a pH-sensitive and tough hydrogel composed of poly(1-  
800 vinylimidazole-*co*-acrylic acid) (P(VI-*co*-AAc)). The formation of intra- and inter-chain  
801 hydrogen bonds between the two monomers endows the gel with significant rigidity and  
802 strength at room temperature in a large range of pH ( $3 \leq \text{pH} \leq 10$ ) (Figure 9a). The high  
803 stability of hydrogen bonds is related to the strength of the proton donor-acceptor pair.<sup>148</sup>  
804 However, the hydrogen bonds can be destructed, either in strongly acidic conditions by  
805 ionization of the imidazole function from VI, or under alkaline conditions with ionization  
806 of the carboxylic group from AAc. In such extreme conditions, the gels become much  
807 weaker. Similar behavior has been reported with other types of gels with strong hydrogen  
808 bonds.<sup>112, 149</sup>

## 809 4.2 Metal-ligand coordinate bonds

810 In a coordinate bond, two electrons from one atom are supplied to a second atom to  
811 generate the interaction. Many parameters, such as the electron-donating ability of the  
812 ligand and the empty orbital of the central metal, govern the strength of the coordinate  
813 bond. Similar to hydrogen bonds, metal-ligand coordinate bonds are typically vulnerable  
814 to pH modifications as it dramatically changes the electron density of ligands or metals.

815 For instance, the ionization of carboxylic groups and the nature of coordination states  
816 (mono-, bis-, or tris-ligand-metal complexes) are very sensitive to the pH environment,  
817 which results in a variation of the association constants of carboxyl-Fe<sup>3+</sup> chelates.<sup>37, 150</sup>

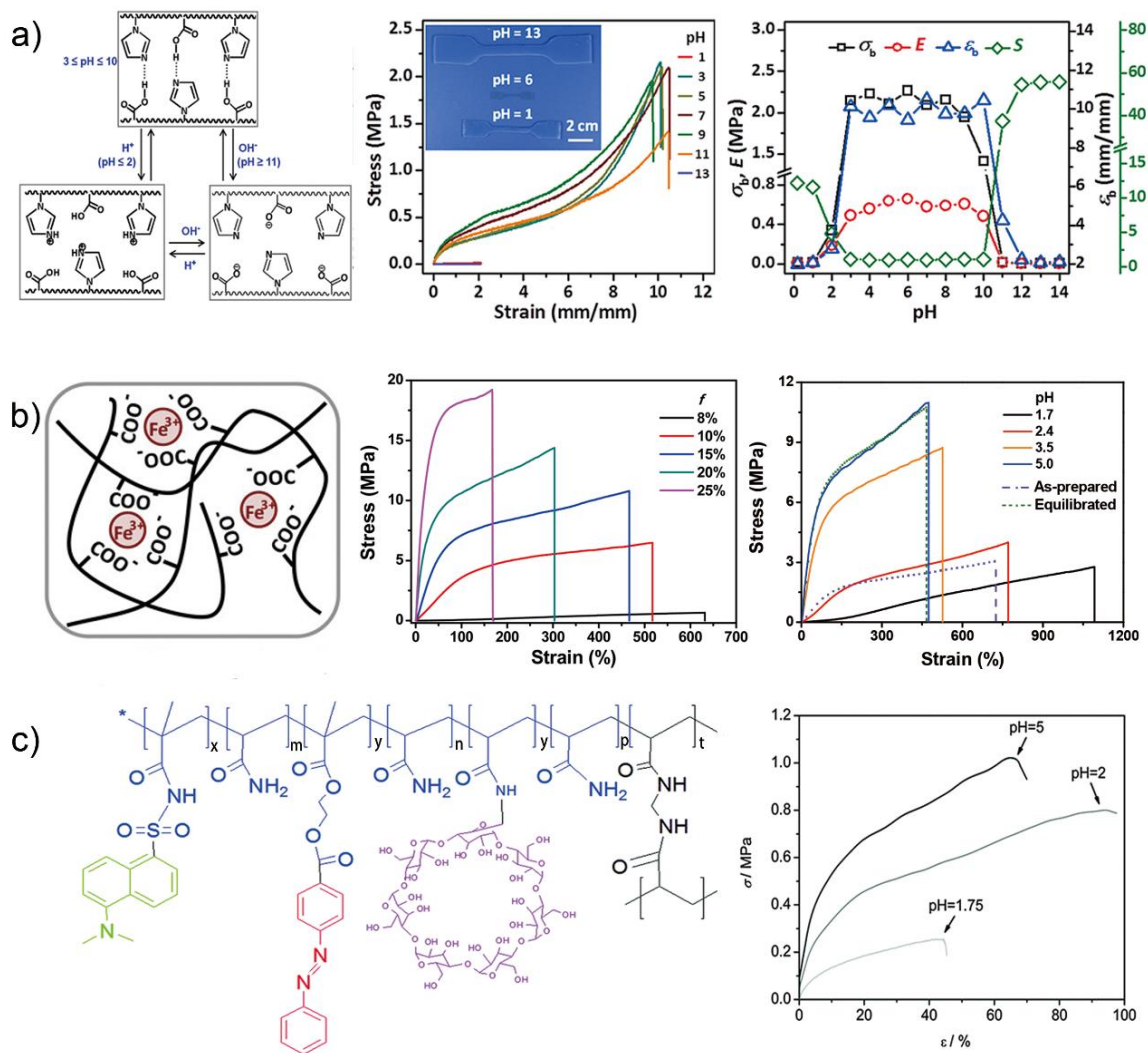
818 Under weak acidic conditions (pH = 4-5), the tris-carboxyl-Fe<sup>3+</sup> coordinate with the  
819 highest stability constant dominates the association behavior and gives rise to the highest  
820 stress at break ( $\sigma_b$ ; see Figure 9b), Young's modulus and extension work. On the other hand,  
821 in more acidic environments (pH = 1.7-3.5), the swelling of the gels increases slightly,  
822 while their mechanical properties decrease sharply, indicating the partial destruction of the  
823 coordination complexes. Under extreme conditions, gels dissolve in highly acidic medium  
824 (pH $\leq$ 1) and disintegrate in alkaline solutions (pH $\geq$ 12), forming ferric hydroxide  
825 precipitates.<sup>35</sup> Analogous carboxylic coordination complexes have been reported with other  
826 metals like Zr<sup>4+</sup>,<sup>151</sup> Cu<sup>2+</sup>,<sup>152</sup> Ag<sup>+</sup>,<sup>153</sup> and Ca<sup>2+</sup>.<sup>152, 154</sup> For all these hydrogels, the mechanical  
827 behavior remains closely related to the nature of the metal and that of the ionizable ligand,  
828 as the stability of the coordinate bond strongly depends on the size of the cations.<sup>154</sup>

### 829 4.3 Osmotic pressure change

830 In addition to the dynamic binding mechanisms mentioned above, when hydrogels carrying  
831 ionizable groups are exposed to acidic or alkaline conditions, they can undergo large  
832 variations in volume which strongly impact the mechanical performance.<sup>144, 146</sup> In the case  
833 of PAAc hydrogels for example, the low level of swelling at low pH induced by the  
834 formation of hydrogen bonds between carboxyl groups makes the gels rather rigid and  
835 stable. Then, by increasing the pH above the pKa, the transformation of -COOH groups  
836 into carboxylate and counterions breaks the hydrogen bonds and generates a strong osmotic  
837 pressure leading to highly swollen and very soft gels which may eventually undergo  
838 autolysis. Although this is the general trend for weak polyelectrolytes up to moderate  
839 swelling, i.e. a Gaussian stretching regime characterized by a decrease of the modulus upon  
840 swelling, an abrupt upturn associated with non-Gaussian elasticity is observed for  
841 extremely larger swelling ratio  $> 100$ ), i.e. smaller polymer volume fraction ( $\phi_2 < 0.01$ ).<sup>155</sup>  
842 For the same reasons, the protonation at low pH of the nitrogen atom of dansyl groups,  
843 introduced by copolymerization within PAAm hydrogels, increases the swelling ratio by  
844 generating high osmotic pressure and therefore make the gels much softer and less  
845 stretchable.<sup>156</sup> Then, when the pH increases above pKa, the deprotonated and hydrophobic  
846 dansyl groups self-associate and act as dynamic crosslinks which improve the toughness  
847 of dansyl-based hydrogels (Figure 9c). Together with the pH and thermo-responsiveness  
848 induced by the host-guest complexes, the materials exhibit a triple-shape memory

849 performance.

850 Although pH is testified as an effective trigger for tuning the mechanical properties of  
851 hydrogels, it is worth mentioning that this environmental trigger is less attractive compared  
852 to temperature and light. One of the main reasons is that the response time is longer since  
853 it requires the diffusion of solutes and solvent within the network and the volume variation  
854 is generally quite large. Indeed, the rate of swelling, which is intrinsically linked to the  
855 collective diffusion coefficient of the polymer, is also influenced by the characteristics of  
856 the sample itself; in particular its size, shape, and porosity.<sup>157</sup> Another disadvantage of the  
857 pH stimulus comes from implementation issues, which generally require a specific liquid  
858 exchange to trigger the mechanical response.



859

860 **Figure 9. pH-responsive hydrogels with tunable mechanical properties. a) Schematic illustration**

861 **of the state of hydrogen bonds in poly(1-vinylimidazole-co-acrylic acid) (P(VI-co-AAc)) hydrogel**

862 **equilibrated in aqueous solutions of different pH and their corresponding mechanical properties.**

863 **Reproduced with permission.<sup>148</sup>. Copyright 2017 Elsevier Ltd. b) Schematic representation of**

864 **ligand-metal complexes formed uniaxial tensile properties of  $\text{Fe}^{3+}$  ions and poly(acrylic acid-co-**

865 **acrylamide) (P(AAm-co-AAc)- $\text{Fe}^{3+}$ ) hydrogels with different feed ratios of AAc. The mechanical**

866 **properties of hydrogels with AAc feed ratio of 15 mol% incubated in solutions at different pH are**

867 **shown on the right side. Reproduced from<sup>35</sup> Copyright 2016 American Chemical Society. c)**

868 **Chemical structure and uniaxial tensile properties of PAAM-based copolymeric hydrogels with**

869 **dansyl side chains at different pH. The x, y and t are 10%, 6%, 10%, respectively. Chemical**

870 structure slightly modified for better presenting the azobenzene group. Reproduced with  
871 permission.<sup>156</sup> Copyright 2016 The Royal Society of Chemistry.

872

## 873 **5. Salt-responsive hydrogels**

874 In nature, inorganic ions are involved in numerous tasks. For instance, the influx of sodium  
875 ions into the cytoplasm and the diffusion of calcium ions into muscle fibers lead to the  
876 contraction of our muscles. Mimicking nature, hydrogels may undergo mechanical change  
877 when in the presence of inorganic salt. Indeed, the salt may play versatile functionalities in  
878 tuning hydrogels' rigidity, including affecting coordinate bonds, impacting polymer  
879 solubility, shielding ionic bonds, and controlling osmotic pressure.

### 880 5.1 Influence of coordinate bonds

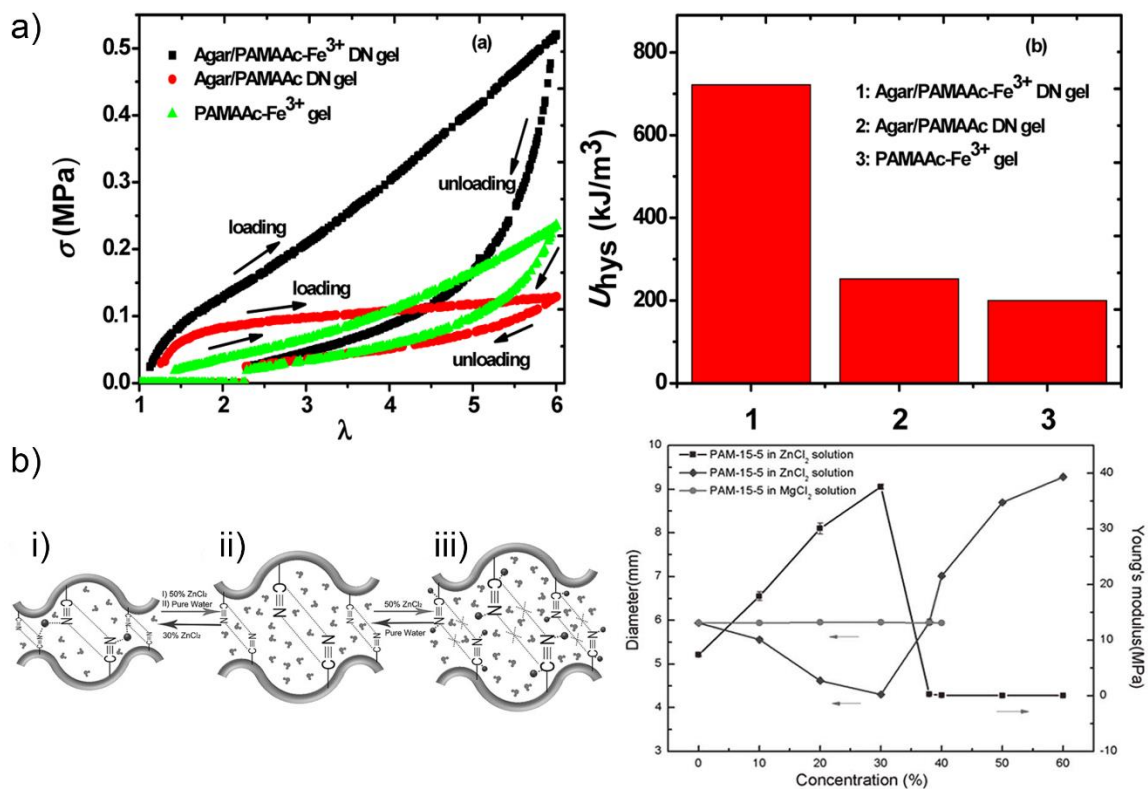
881 In chemistry, coordinate bonds typically involve the binding of a metal to certain ligands  
882 such as carboxylate-ions to form coordination complexes. These coordination complexes  
883 are of both academic and practical interest. In the case of hydrogels having a certain amount  
884 of coordinate sites, the introduction of suitable transition metal ions can give rise to the  
885 formation of new crosslinking points and effectively affect the mechanical performance of  
886 the hydrogels. It should be noted that the toughening process induced by the formation of  
887 strong metal-coordinate bonds is limited to specific ion pairs, which can be generally  
888 explained by the classical hard-soft acid-base theory postulating that hard acids bind

889 strongly to hard bases and soft acids strongly bind to soft bases.<sup>158</sup>

890 As a representative example, Chen et al.<sup>159</sup> introduced  $\text{Fe}^{3+}$  into a double network gel  
891 consisting of an agar gel, as the first physical network, embedded into a chemically  
892 crosslinked second network of P(AAm-*co*-AAc) (PAMAAC). Besides the pH-tunable  
893 performance derived from the AAc group, the gel demonstrates significant ion-  
894 responsiveness. Compared to the gels without  $\text{Fe}^{3+}$ , Agar/PAMAAC- $\text{Fe}^{3+}$  gels demonstrate  
895 an enhancement of fracture stress and hysteresis energy by 3.4 times and 2.8 times,  
896 respectively (Figure 10a). The large amplitude of the hysteresis comes from the unzipping  
897 of the additional physical network of coordinate complexes.<sup>160</sup> Therefore, the formation of  
898 reversible sacrificial ionic crosslinks appears as an interesting strategy to reinforce gel  
899 properties by simply immersing polycarboxylic acid hydrogel into a suitable multivalent  
900 salt solution.<sup>161</sup>

901 Metal ions can also significantly affect hydrogels' toughness by forming different dentate  
902 ligands in coordination compounds;<sup>162</sup> the mechanical properties being influenced by the  
903 immersing time as well as the ion concentration. For example, poly(acrylonitrile-*co*-2-  
904 methacryloyloxyethyl phosphorylcholine) (P(AN-*co*-MPC)) hydrogels, designed with  
905 dipole-dipole interactions between cyano groups (CN-CN pairs) and coordinate bonds  
906 between CN and  $\text{Zn}^{2+}$  ions, were developed by Han et al.<sup>34</sup> As shown in Figure 10b, the  
907 hydrogel, which is initially reinforced by the strong CN-CN interactions within the network,

908 shrinks progressively when immersed in  $\text{ZnCl}_2$  solutions as zinc ions may serve as  
909 additional physical crosslinks between cyano groups due to favorable formation of  
910  $\text{Zn}(\text{CN})_2$ . Concurrently, the Young modulus increases from 7 MPa, initially in water, up to  
911 38 MPa in 30%  $\text{ZnCl}_2$  solution. Then, when the zinc ion concentration is increased beyond  
912 30%, excessive zinc ions bind to single CN groups and shield other cyano groups from  
913 forming dipole-dipole interactions. In this range of concentrations ( $[\text{ZnCl}_2] > 38\%$ ), the gel  
914 highly swells and its Young's modulus sharply decreases up to 0.05 MPa in 50 %  $\text{ZnCl}_2$ .  
915 Therefore, by adjusting the concentration of  $\text{ZnCl}_2$  in the external solution, the authors  
916 demonstrate that the elastic modulus of the gel can be tuned over a very wide range, from  
917 kPa to MPa, allowing shape memory properties to be developed with various temporary  
918 and permanent shapes.



919

920 **Figure 10. Mechanism and mechanical properties of hydrogels with salt-responsiveness. a)**

921 **Loading-unloading curves and the corresponding dissipated energies of Agar/PAMAAc-Fe<sup>3+</sup> DN**

922 **gel, Agar/PAMAAc DN gel, and PAMAAc-Fe<sup>3+</sup> gel. Reproduced from<sup>159</sup> Copyright 2016 American**

923 **Chemical Society. b) Schematic representation of 3 different hydrogel states featuring: i) CN-CN**

924 **+ CN-Zn interactions, ii) CN-CN interactions and iii) dissociation of the previous interactions of**

925 **poly(acrylonitrile 2-methacryloyloxyethyl phosphorylcholine) hydrogel (named PAM in the figure)**

926 **in response to zinc ions. On the right side, the figure shows the variation of Young's modulus**

927 **(square  $\square$ ) and the diameter (diamond  $\diamond$ ) of the gel for different concentrations of ZnCl<sub>2</sub> (MgCl<sub>2</sub>**

928 **solution serves as a control). Reproduced with permission.<sup>34</sup> Copyright 2012 WILEY-VCH Verlag**

929 **GmbH & Co. KGaA, Weinheim.**

930

931 Similar performances have been demonstrated in polycarboxylate systems with other metal

932 ions including  $\text{Ca}^{2+}$ ,<sup>152, 154, 161, 163-164</sup>  $\text{Al}^{3+}$ ,<sup>163</sup> and  $\text{Cu}^{2+}$  ions<sup>152</sup>. Such behaviors are highly  
933 related to the type of central metal and ionizable ligand, as the bond stability fundamentally  
934 scales with the decreasing size of the cation.<sup>154</sup> Moreover,  $\text{Zr}^{4+}$  ions which are known to  
935 form coordinate bonds with sulfonate groups, can effectively reinforce such hydrogels.<sup>165</sup>  
936 For instance, the immersion of a poly(acrylamide-*co*-2-acrylamido-2-methyl-1-  
937 propanesulfonic acid) (P(AAm-*co*-AMPS)) hydrogel into a  $\text{ZrOCl}_2$  solution gives rise to  
938 an enhancement in fracture stress of 3 orders of magnitude (from 2.5 kPa to 6.3 MPa).  
939 Upon stretching, the sulfonate- $\text{Zr}^{4+}$  coordination complexes can break, dissipating energy,  
940 and reform, ensuring satisfactory mechanical performance. Owing to the dynamic nature  
941 of the coordinate bonds, these hydrogels show rate- and temperature-dependent mechanical  
942 performances, as well as good self-recovery properties. These hydrogels enable versatile  
943 applications in the biomedical and engineering fields, such as artificial tubular grasper.

## 944 5.2 Solubility effect

945 Besides the aforementioned mechanisms, salt can also modify the characteristics of  
946 hydrogels by affecting the polymer/water interactions. Historically, Hofmeister was the  
947 first to report that the water solubility of proteins could be increased or decreased in a  
948 controlled manner by adjusting the nature and concentration of the salt. Nowadays, the  
949 ranking of the physical properties of ions in aqueous solutions, known as Hofmeister series,  
950 is a benchmark widely used to modify the solubility of polymers and smaller molecules in

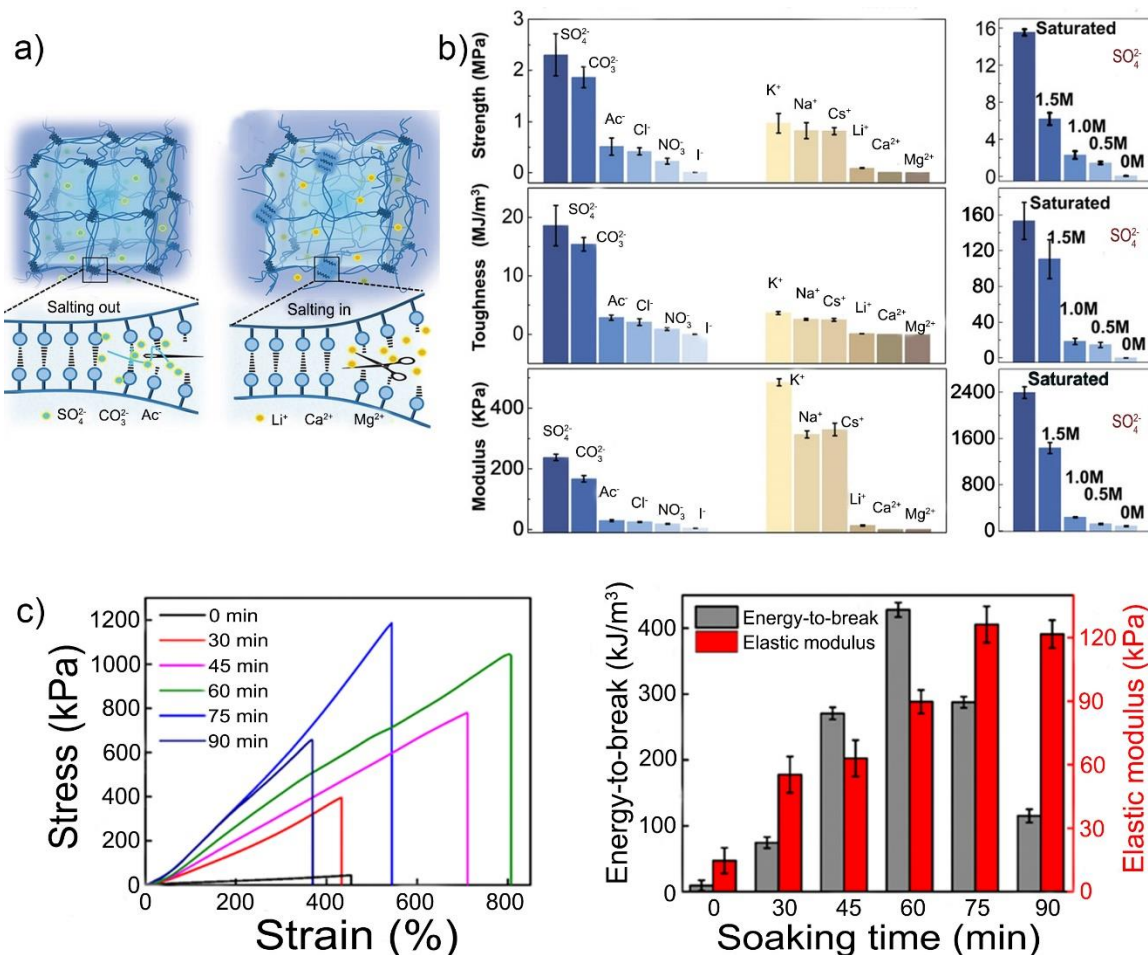
951 water.<sup>166</sup> Although the underlying mechanisms are still under debate after more than one  
952 century, hydrogen bonding, dispersion interactions, hydration forces, or even dissolved gas  
953 have been suggested for this phenomenon.<sup>167</sup> In the case of PNIPAm gels, for which  
954 interactions in water result from a compromise between hydrogen bonds and hydrophobic  
955 interactions, the transition temperature as well as the macroscopic properties can be finely  
956 tuned by applying the so-called Hofmeister effects.<sup>168</sup>

957 In the Hofmeister series, ions are divided into “kosmotropes” and “chaotropes” with  
958 salting-out and salting-in effects, respectively, indicating how the interactions of small  
959 solute molecules with water affect the solubility of large molecules.<sup>169</sup> While the salting-  
960 out effect tends to reduce the hydration of polymer chains,<sup>170</sup> strengthen specific physical  
961 interactions,<sup>171</sup> and consequently reinforce the mechanical behavior of hydrogels, the  
962 salting-in leads to opposite effects. In the work of Chen and co-authors,<sup>172</sup> the mechanical  
963 properties of poly(acrylamide)/methylcellulose (PAAm/MC) hydrogels were significantly  
964 improved by simply soaking the gel in solutions of kosmotropic ions. By increasing the  
965 hydrophobic interactions, the small kosmotropic anions thus led to chain bundling,  
966 endowing the hydrogels with enhanced mechanical properties. For instance, the tensile  
967 strength of the treated hydrogel reached as high as 4.4 MPa, which is more than 30 times  
968 higher than that of the original hydrogel. Upon stretching, these hydrophobic associations  
969 readily break, dissipating energy, and then reform guaranteeing good mechanical  
970 performance. Following this strategy, the mechanical properties of these hydrogels can be

971 further tuned by varying the post soaking time and the kind of Hofmeister salts. The  
972 PAAm/MC hydrogels treated with solutions of strong “salting-out” anions like  $\text{Cit}^{3-}$ ,  $\text{CO}_3^{2-}$   
973 and  $\text{SO}_4^{2-}$ , reached higher compression strength of 27.6, 19.6, and 14.2 MPa, respectively.  
974 In comparison, the same gel immersed in a solution containing a weak “salting-out” anion  
975 ( $\text{Cl}^-$ ) exhibits a much weaker fracture compression stress (7.4 MPa). While the high  
976 mechanical performance of this hydrogel is maintained in saline solution, the hydrogel  
977 swells and loses its mechanical strength when immersed in pure water.<sup>172</sup> Very recently, He  
978 and coauthors attested that the mechanical properties of poly(vinyl alcohol) (PVA)  
979 hydrogels can be well-tuned at a broad range by simply soaking the as-prepared gels in  
980 different ions solutions.<sup>173</sup> As shown in Figure 11a, hydrogen bonds forming or breaking  
981 can be induced by ions due to the salting-out effect or salting-in effect. With different media  
982 soaked, the PVA hydrogels demonstrate tensile strength from 50 kPa to 15 MPa, toughness  
983 from 0.0167 to 150  $\text{MJ m}^{-3}$ , and Young’s modulus from 24 to 2500 kPa (Figure 11b). It is  
984 verified that the Hofmeister effect accounts for this phenomenon by affecting the  
985 aggregation states of the polymer chains and the formation of structures, rather than just  
986 affecting the hydration level or playing a role as the components of hydrogels. The  
987 Hofmeister effect becomes more pronounced with crystalline hydrogels as the salt also  
988 affect the crystalline degree in PVA hydrogels.<sup>174</sup>

989 The salt-sensitive mechanical response of hydrogels can also be finely adjusted by simply  
990 controlling the immersion time. Cui et al.<sup>175</sup> have developed chitosan/poly(acrylic acid)

991 double network nanocomposite hydrogels (CS/PAA/TA@CNC) via in situ polymerization  
992 of acrylic acid in chitosan acid aqueous solution with tannic acid-coated cellulose  
993 nanocrystal acting as nanofillers. These nanocomposite hydrogels were then soaked into a  
994 saturated NaCl solution in order to aggregate chitosan chains by shielding electrostatic  
995 repulsions between positively charged amino groups. Compared with the original hydrogel,  
996 without soaking treatment, the “CS/PAA/TA@CNC-60” gel, which was immersed for 60  
997 min in a saturated NaCl solution, exhibits a significant enhancement of the mechanical  
998 properties with a 10-fold increase in the fracture stress and a 2-fold increase in the fracture  
999 strain, which is attributed to a higher crosslinking density of chitosan induced by chain  
1000 entanglement and salting-out effect (Figure 11c). With further extended soaking time, the  
1001 fracture energy and elastic modulus began to decrease due to excessive shielded  
1002 electrostatic repulsions, which has another salt effect will be discussed in the following  
1003 part.



1004

1005 **Figure 11. Mechanism and mechanical properties of hydrogels with Hofmeister effect. a)**  
 1006 **Hydrogen bonds form or break between PVA polymer chains induced by ions due to salting-out**  
 1007 **or salting-in effect. b) Strengths, toughness, and moduli of PVA hydrogels tuned by various anions**  
 1008 **(with Na<sup>+</sup> as the constant counterion); different cations (with Cl<sup>-</sup> as the constant counterion); and**  
 1009 **Na<sub>2</sub>SO<sub>4</sub> with concentrations ranging from 0 m to saturated. Reproduced with permission.<sup>173</sup>**  
 1010 **Copyright 2021 Wiley-VCH GmbH. c) Tensile stress–strain curves, elastic modulus, and energy-**  
 1011 **to-break of the tannic acid-coated cellulose nanocrystal CS/PAA/TA@CNC DN nanocomposite**  
 1012 **hydrogels with different soaking time in saturated NaCl solution. Reproduced from<sup>175</sup>. Copyright**  
 1013 **2019 American Chemical Society.**

1014

### 1015 5.3 Shielding of ionic interactions

1016 In hydrogels, ionic interactions greatly contribute to strengthening their properties. Upon  
1017 stretching, these noncovalent bonds can reversibly break to dissipate energy and reform to  
1018 guarantee their mechanical performance and stability. Consequently, the addition of small  
1019 molecular salts can effectively screen the attractive interactions between oppositely  
1020 charged groups carried by macromolecular chains, leading to the release of entangled  
1021 polymer chains.<sup>39, 175</sup>

1022 Polyampholytes (PA) hydrogels, containing both anions and cations in their  
1023 macromolecular structure, are typical examples of materials sensitive to salt additives due  
1024 to electrostatic screening. In the pioneering work of Gong et al.,<sup>176</sup> PA hydrogels were  
1025 prepared with an equal amount of the 3-(methacryloylamino) propyl-trimethylammonium  
1026 chloride (MPTC, cationic monomer) and sodium p-styrenesulfonate (NaSS, anionic  
1027 monomer). Close to the charge balance in pure water, these hydrogels display extremely  
1028 high toughness with remarkable viscoelasticity which is attributed to the very wide  
1029 distribution of ionic bond strengths. The strong bonds serve as permanent crosslinks,  
1030 imparting elasticity, while the weak bonds reversibly break and reform, dissipating energy.  
1031 However, the addition of inorganic salt gradually weakens the strength of electrostatic  
1032 interactions and leads to a significant decrease in Young's modulus (from 2.2 to 0.1 MPa)  
1033 and fracture stress  $\sigma_b$  (from 2.60 to 0.07 MPa). Unlike the intrachain ionic complexation  
1034 that takes place in PA hydrogels, polyion complex (PIC) hydrogels prepared from equal

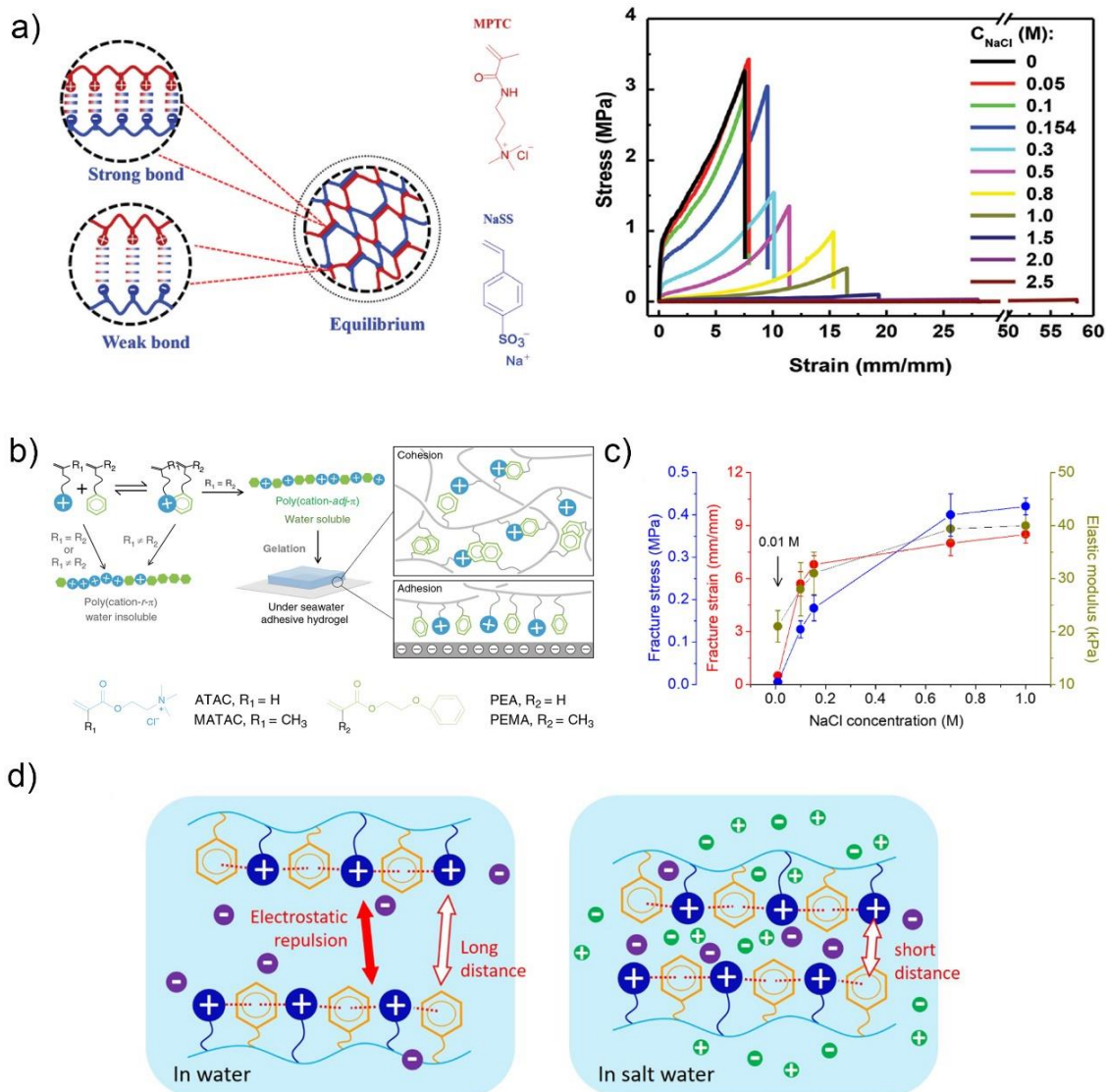
1035 oppositely charged homo-polyelectrolytes can only lead to interchain complexation  
1036 between polymers in the extended coil conformation. This interchain complexation, which  
1037 takes place even at low polymer concentrations, greatly promotes the chain entanglement  
1038 and the stability of ionic complexes, thus making the mechanical properties much superior  
1039 to those of PA hydrogels with the same rate of combination of monomers. When these PIC  
1040 hydrogels synthesized from MPTC and NaSS homopolymers are immersed in saline  
1041 solutions of increasing concentration, a decrease in the breaking stress as well as a  
1042 significant increase in fracture strain are observed (Figure 12a).<sup>177</sup> By tuning the screening  
1043 of interpolymer electrostatic interactions with salt, it is possible to control the dynamics of  
1044 ionic bonds and endow the hydrogel with self-healing properties. For instance, after  
1045 soaking two pieces of hydrogels for 2 minutes in 3M NaCl and bringing them into contact  
1046 for 12 hours at room temperature, the self-healed sample exhibits a recovery rate of 66 %  
1047 in terms of work of extension with high strength (modulus ~ 4.5 MPa; fracture stress ~ 2.2  
1048 MPa; fracture strain ~ 630%).

#### 1049 5.4 Controlling osmotic pressure

1050 In hydrogels, water plasticizes polymers by disrupting chain interactions, creating free  
1051 volume in the polymer network, enhancing chain mobility, and softening the material. The  
1052 ionic contribution to the osmotic pressure has a huge effect on the swelling properties of  
1053 gels and it can be used either to generate super swelling properties, as in superabsorbent  
1054 polymers or to cause the gel collapsing when the excess of ionic pressure inside the network

1055 is counterbalanced by that of the external environment with the addition of salt. Such  
1056 osmotic deswelling, which increases the density of polymer chains in the network, also  
1057 participates in strengthening the specific physical interactions.

1058 This phenomenon has been particularly investigated in ionic gels using additional  
1059 noncovalent associations as nicely exemplified by Gong and coworkers who couple  
1060 electrostatic and hydrophobic interactions within the same network.<sup>178</sup> As shown in Figure  
1061 12b, the authors synthesized copolymers through cation- $\pi$  complex-aided free-radical  
1062 polymerization between an aromatic monomer and a cationic one. While the copolymer  
1063 itself is water-soluble, due to electrostatic repulsions between the chains dominating the  
1064 solution behavior, the addition of salt favors the formation of a gel coacervate as salt ions  
1065 screen long-range electrostatic repulsions and strengthen the effective cation- $\pi$  and  
1066 hydrophobic interactions taking place intra- and inter-molecularly (Figure 12c). While the  
1067 copolymer solution prepared in pure water is not sufficiently elastic to be able to withstand  
1068 deformation, the system becomes much harder and more stretchable in salty environments  
1069 (Figure 12d). Such materials, which are also characterized by self-healing and adhesive  
1070 properties in saline conditions, are promising systems paving the way for the development  
1071 of responsive hydrogels in physiological and marine environments.



1072

1073 **Figure 12. Salt-sensitive hydrogels with shielding of ionic interactions and controlling osmotic**  
 1074 **pressure. a) Schematic illustration of PIC hydrogels prepared from poly(3-(methacryloylamino)**  
 1075 **propyl-trimethylammonium chloride) (MPTC) and poly(sodium p-styrenesulfonate) (NaSS) and**  
 1076 **uniaxial performance in response to immersion in different NaCl solutions. The chemical**  
 1077 **structure of corresponding monomers is illustrated on the left side. Reproduced with**  
 1078 **permission.<sup>177</sup> Copyright 2015 WILEY-VCH Verlag GmbH & Co. KGaA, Weinheim. b)**  
 1079 **Schematic illustration of design strategy with chemical structures of typical monomers used, c)**  
 1080 **fracture stress, fracture strain and elastic modulus obtained from stress-strain curves with**

1081 **P(ATAC-adj-PEA) gels, and d) schematic illustration of the formation of coacervate in saltwater.**  
1082 **Reproduced with permission.<sup>178</sup> Copyright 2019 Nature.**

1083

1084 As already discussed, the introduction of salt which will favor the formation of physical-  
1085 crosslinked domains largely contributes to the energy dissipation and endow the gels with  
1086 reinforced mechanical performance.<sup>179</sup> Using the simple soaking process, salt-responsive  
1087 hydrogels prepared from natural or synthetic macromolecules can be easily strengthened  
1088 for use in versatile applications, such as bone regeneration,<sup>33</sup> tubular graspers,<sup>165</sup> sensors.<sup>175</sup>  
1089 Nevertheless, as discussed in the case of pH-sensitive hydrogels, the time required for the  
1090 solutes to diffuse within the gel can be a significant obstacle for some practical applications.

## 1091 **Conclusion and perspective**

1092 Over the past 4 decades, hydrogels with responsive properties have been definitively a hot  
1093 topic with significant academic developments. Until the 1990s, researchers mainly focused  
1094 on the thermodynamic aspects of the volume phase transition of hydrogels in response to  
1095 environmental stimuli, and many new and complex architectures have been designed and  
1096 studied within this framework. Since the beginning of the new century, the vast knowledge  
1097 acquired on these systems, as well as the development of experimental techniques, have  
1098 led to direct research towards the mechanical properties of hydrogels in order to elaborate  
1099 smart and efficient reinforcement strategies. This new orientation, stimulated in particular  
1100 by the potential of these swollen materials in biomedical applications, has led to a

1101 multiplication and a sophistication of the systems studied, making it possible to consider  
1102 the control of their mechanical properties using single or multiple environmental triggers.  
1103 Today, there is a truly solid basis of knowledge for the structure/properties relationships of  
1104 smart hydrogels characterized by responsive mechanical properties under thermal, light,  
1105 pH, and/or salt triggers, but improvements are needed and we have still a lot to learn from  
1106 nature.

1107 In the case of stimuli-responsive gels, not only thermodynamics prevails but also kinetic  
1108 aspects play an important role at different scales that must be considered in the transition  
1109 process. On the one hand, the rate of thermal transfer is faster compared to the other  
1110 processes (e.g.  $2\text{-}3\cdot 10^{-3}\text{ cm}^2\cdot\text{s}^{-1}$  for PNIPAm). On the other hand, the transport rate of  
1111 solvent or solute into or out of the network is much slower. In the case of a purely diffusive  
1112 mechanism, the experimental values measured in the gels are close to the self-diffusion  
1113 coefficients of the molecules (e.g.  $2.6\cdot 10^{-5}\text{ cm}^2\cdot\text{s}^{-1}$  for  $\text{D}_2\text{O}$ ). Moreover, the movement of  
1114 polymer chains further limits the kinetic process in the case of large volume phase  
1115 transition. On average, the collective diffusion coefficient for a homogeneous gel is around  
1116 2 orders of magnitude lower compared to the solvent and 4 orders compared to the thermal  
1117 stimulus. In particular, this factor will be the limiting step of the kinetic process in the case  
1118 of large volume phase transition, keeping in mind that the characteristic swelling time ( $\tau$ )  
1119 scales with the square of the size of the sample ( $r$ ) as:  $\tau \sim r^2/D_0$ . Such kinetic issues can  
1120 be critical in the case of pH and/or salt responsive toughening, where environmental

1121 modifications should be driven by soaking the gel in an external medium and waiting for  
1122 minutes or even hours depending on the size of the sample. This is rather long compared  
1123 to hydrogels found in the human body that display much shorter characteristic times on the  
1124 order of a second or less. Photo-stimulation is an alternative a good way to overcome the  
1125 problems associated with the slow diffusion of solutes into the gel, but the short  
1126 penetrability of light remains a critical issue. Another problem that deserves to be pointed  
1127 out concerns the sensitivity of the gel to a stimulus. Indeed, while in nature an infinitesimal  
1128 change in biological signals can induce a significant mechanical response, synthetic  
1129 responsive hydrogels require a greater variation in environmental conditions to provide a  
1130 macroscopic response. In addition, the lack of reversibility of some responsive hydrogels  
1131 also limits their long-term use.

1132 With an increasing understanding of the structure/property relationships of these soft and  
1133 wet materials, new versatile systems will certainly emerge in the future. On the one hand,  
1134 an increasing number of smart hydrogels whose mechanical performances are responsive  
1135 to novel stimuli may come on the scene, e.g. the electrical, magnetic, touch, or  
1136 electrochemical triggers. These input signals are ubiquitous in bio-tissues, such as our  
1137 central nervous system takes the art of electrochemistry for nerve conduction and muscle  
1138 movement control. Different from currently applied triggers, these new stimuli may safely  
1139 overcome the existing problem of low responsive time. Although hydrogels with such  
1140 stimuli become increasingly valued in recent years, the related researches are still in their

1141 infancy compared to the real cases in nature. On the other hand, new hydrogels with  
1142 stimuli-responsive mechanical performance may appear with a super-low threshold value.  
1143 Furthermore, the gels may even become capable to differentiate between similar inputs.  
1144 These perspectives are highly challenging for existing hydrogels but out of question in the  
1145 biological world. For example, the motion of our smooth muscle is closely associated with  
1146 very tiny environmental pH variation and the physiological effect of sodium and potassium  
1147 ions are poles apart. Another important issue is how to create hydrogels with step-by-step  
1148 regulation in mechanical performance. Taking the *Mimosa Pudica* for illustration: upon  
1149 touching, the plant experiences stimulus perception at first, giving rise to electrical signal  
1150 transmission in the next and finally induces rapid mechanical movement. The more intense  
1151 the stimuli, the longer it takes to maintain the closing state. The advantage of this cascade  
1152 system is that it is able to produce fast, delicate, adaptive, and reversible mechanical output.  
1153 Nevertheless, there is still a certain distance before obtaining this kind of artificial soft  
1154 matter.

1155 Indeed, after 40 years of intensive studies on responsive hydrogels, we have learned a lot  
1156 about how to use physical interactions to control the macroscopic response of the hydrogel  
1157 and in particular how to modulate the mechanical properties. Although we still have a long  
1158 way to go by learning from nature, the weaknesses of current hydrogels will be the next  
1159 milestones for future research with an increasing focus on practical applications in the near  
1160 future.

1161 AUTHOR INFORMATION

1162 **Corresponding authors**

1163 E-mail: [guoh37@mail.sysu.edu.cn](mailto:guoh37@mail.sysu.edu.cn) (H. G.);

1164 E-mail: [dominique.hourdet@espci.fr](mailto:dominique.hourdet@espci.fr) (D. H.)

1165 **ORCID:**

1166 Xiaolin Wang: 0000-0002-2870-1111

1167 Zi Liang Wu: 0000-0002-1824-9563

1168 Hui Guo: 0000-0002-4652-2395

1169 Dominique Hourdet: 0000-0002-0328-7014

1170 **Author Contributions**

1171 †These authors contribute equally to this work.

1172 **Notes**

1173 The authors declare no conflict of interest.

1174

1175 ACKNOWLEDGMENT

1176 The authors gratefully acknowledge the financial support from the National Natural

1177 Science Foundation of China (NSFC) (No. 51903253), Natural Science Foundation of

1178 Guangdong Province of China (2019A1515011150, 2019A1515011258), and the Science

1179 and Technology Development Fund of Macao (FDCT 0009/2019/A, 0083/2019/A2,

1180 0007/2019/AKP).

1181 REFERENCES

- 1182 (1) Montero de Espinosa, L.; Meesorn, W.; Moatsou, D.; Weder, C. Bioinspired Polymer  
1183 Systems with Stimuli-Responsive Mechanical Properties. *Chem. Rev.* **2017**, *117*, 12851-  
1184 12892.
- 1185 (2) Zhang, D.; Ren, B.; Zhang, Y.; Xu, L.; Huang, Q.; He, Y.; Li, X.; Wu, J.; Yang, J.; Chen,  
1186 Q.; Chang, Y.; Zheng, J. From design to applications of stimuli-responsive hydrogel strain  
1187 sensors. *J. Mater. Chem. B* **2020**, *8*, 3171-3191.
- 1188 (3) Ebara, M.; Kotsuchibashi, Y.; Uto, K.; Aoyagi, T.; Kim, Y.-J.; Narain, R.; Idota, N.;  
1189 Hoffman, J. M. Smart Hydrogels. In *Smart Biomaterials*; Springer: Tokyo, 2014; pp 9-65.
- 1190 (4) Vijay Kumar Thakur, M. K. T. Hydrogels. In *Gels Horizons: From Science to Smart*  
1191 *Materials*; Vijay Kumar Thakur, M. K. T., Ed.; Springer Singapore: Singapore, 2018.
- 1192 (5) Wang, X.; Ronsin, O.; Gravez, B.; Farman, N.; Baumberger, T.; Jaisser, F.; Coradin, T.;  
1193 H elary, C. Nanostructured Dense Collagen-Polyester Composite Hydrogels as Amphiphilic  
1194 Platforms for Drug Delivery. *Adv. Sci.* **2021**, *8*, 2004213.
- 1195 (6) Qiu, Y.; Park, K. Environment-sensitive hydrogels for drug delivery. *Adv. Drug Deliv.*  
1196 *Rev.* **2012**, *64*, 49-60.
- 1197 (7) Yang, C.; Suo, Z. Hydrogel ionotronics. *Nat. Rev. Mater.* **2018**, *3*, 125-142.
- 1198 (8) Yuk, H.; Lu, B.; Zhao, X. Hydrogel bioelectronics. *Chem. Soc. Rev.* **2019**, *48*, 1642-  
1199 1667.
- 1200 (9) Qin, H.; Zhang, T.; Li, N.; Cong, H. P.; Yu, S. H. Anisotropic and self-healing hydrogels  
1201 with multi-responsive actuating capability. *Nat. Commun.* **2019**, *10*, 2202.
- 1202 (10) Taylor, D. L.; in het Panhuis, M. Self-Healing Hydrogels. *Adv. Mater.* **2016**, *28*, 9060-  
1203 9093.
- 1204 (11) Ke, Y.; Chen, J.; Lin, G.; Wang, S.; Zhou, Y.; Yin, J.; Lee, P. S.; Long, Y. Smart  
1205 Windows: Electro - , Thermo - , Mechano - , Photochromics, and Beyond. *Adv. Energy*  
1206 *Mater.* **2019**, *9*, 1902066.
- 1207 (12) Liu, X.; Liu, J.; Lin, S.; Zhao, X. Hydrogel Machines. *Mater. Today* **2020**, *36*, 102-  
1208 124.
- 1209 (13) Buwalda, S. J.; Boere, K. W. M.; Dijkstra, P. J.; Feijen, J.; Vermonden, T.; Hennink,  
1210 W. E. Hydrogels in a historical perspective: From simple networks to smart materials. *J.*  
1211 *Control. Release* **2014**, *190*, 254-273.
- 1212 (14) Shintake, J.; Cacucciolo, V.; Floreano, D.; Shea, H. Soft Robotic Grippers. *Adv. Mater.*  
1213 **2018**, *30*, 1707035.
- 1214 (15) Shi, Q.; Liu, H.; Tang, D.; Li, Y.; Li, X.; Xu, F. Bioactuators based on stimulus-  
1215 responsive hydrogels and their emerging biomedical applications. *NPG Asia Mater.* **2019**,  
1216 *11*, 64.

- 1217 (16) Zhou, Y.; Dong, X.; Mi, Y.; Fan, F.; Xu, Q.; Zhao, H.; Wang, S.; Long, Y. Hydrogel  
1218 smart windows. *J. Mater. Chem. A* **2020**, *8*, 10007-10025.
- 1219 (17) Sneddon, I. N.; Berry, D. S. The Classical Theory of Elasticity. In *Elasticity and*  
1220 *Plasticity / Elastizität und Plastizität*; Flügge, S., Ed.; Springer Berlin Heidelberg: Berlin,  
1221 Heidelberg, 1958; pp 1-126.
- 1222 (18) Obukhov, S. P.; Rubinstein, M.; Colby, R. H. Network Modulus and Superelasticity.  
1223 *Macromolecules* **1994**, *27*, 3191-3198.
- 1224 (19) Schröder, U. P.; Oppermann, W. Mechanical and stress-optical properties of strongly  
1225 swollen hydrogels. *Makromol. Chem. Macromol. Symp.* **1993**, *76*, 63-74.
- 1226 (20) Rubinstein, M.; Colby, R. H.; Dobrynin, A. V.; Joanny, J.-F. Elastic Modulus and  
1227 Equilibrium Swelling of Polyelectrolyte Gels. *Macromolecules* **1996**, *29*, 398-406.
- 1228 (21) Maugis, D.; Barquins, M. Fracture mechanics and the adherence of viscoelastic bodies.  
1229 *J. Phys. D: Appl. Phys.* **1978**, *11*, 1989-2023.
- 1230 (22) Lake, G. J.; Lindley, P. B. The mechanical fatigue limit for rubber. *J. Appl. Polym. Sci.*  
1231 **1965**, *9*, 1233-1251.
- 1232 (23) Lake, G. J.; Lindley, P. B. Cut growth and fatigue of rubbers. II. Experiments on a  
1233 noncrystallizing rubber. *J. Appl. Polym. Sci.* **1964**, *8*, 707-721.
- 1234 (24) Creton, C. 50th Anniversary Perspective: Networks and Gels: Soft but Dynamic and  
1235 Tough. *Macromolecules* **2017**, *50*, 8297-8316.
- 1236 (25) Baumberger, T.; Caroli, C.; Martina, D. Fracture of a biopolymer gel as a viscoplastic  
1237 disentanglement process. *Eur. Phys. J. E.* **2006**, *21*, 81-89.
- 1238 (26) Haque, M. A.; Kurokawa, T.; Kamita, G.; Gong, J. P. Lamellar Bilayers as Reversible  
1239 Sacrificial Bonds To Toughen Hydrogel: Hysteresis, Self-Recovery, Fatigue Resistance,  
1240 and Crack Blunting. *Macromolecules* **2011**, *44*, 8916-8924.
- 1241 (27) Zhao, X. Multi-scale multi-mechanism design of tough hydrogels: building dissipation  
1242 into stretchy networks. *Soft Matter* **2014**, *10*, 672-87.
- 1243 (28) Bilici, C.; Ide, S.; Okay, O. Yielding Behavior of Tough Semicrystalline Hydrogels.  
1244 *Macromolecules* **2017**, *50*, 3647-3654.
- 1245 (29) Guo, M.; Pitet, L. M.; Wyss, H. M.; Vos, M.; Dankers, P. Y.; Meijer, E. W. Tough  
1246 stimuli-responsive supramolecular hydrogels with hydrogen-bonding network junctions. *J.*  
1247 *Am. Chem. Soc.* **2014**, *136*, 6969-6977.
- 1248 (30) Nonoyama, T.; Lee, Y. W.; Ota, K.; Fujioka, K.; Hong, W.; Gong, J. P. Instant Thermal  
1249 Switching from Soft Hydrogel to Rigid Plastics Inspired by Thermophile Proteins. *Adv.*  
1250 *Mater.* **2020**, *32*, 1905878.
- 1251 (31) Nakajima, T. Generalization of the sacrificial bond principle for gel and elastomer  
1252 toughening. *Polym. J.* **2017**, *49*, 477-485.
- 1253 (32) Hao, J.; Weiss, R. A. Viscoelastic and Mechanical Behavior of Hydrophobically

- 1254 Modified Hydrogels. *Macromolecules* **2011**, *44*, 9390-9398.
- 1255 (33) Jiang, L. B.; Su, D. H.; Ding, S. L.; Zhang, Q. C.; Li, Z. F.; Chen, F. C.; Ding, W.;  
1256 Zhang, S. T.; Dong, J. Salt - Assisted Toughening of Protein Hydrogel with Controlled  
1257 Degradation for Bone Regeneration. *Adv. Funct. Mater.* **2019**, *29*, 1901314.
- 1258 (34) Han, Y.; Bai, T.; Liu, Y.; Zhai, X.; Liu, W. Zinc ion uniquely induced triple shape  
1259 memory effect of dipole-dipole reinforced ultra-high strength hydrogels. *Macromol. Rapid*  
1260 *Commun.* **2012**, *33*, 225-231.
- 1261 (35) Zheng, S. Y.; Ding, H.; Qian, J.; Yin, J.; Wu, Z. L.; Song, Y.; Zheng, Q. Metal-  
1262 Coordination Complexes Mediated Physical Hydrogels with High Toughness, Stick-Slip  
1263 Tearing Behavior, and Good Processability. *Macromolecules* **2016**, *49*, 9637-9646.
- 1264 (36) Yang, P.; Wang, X.; Fan, H.; Gu, Y. Effect of hydrogen bonds on the modulus of bulk  
1265 polybenzoxazines in the glassy state. *Phys. Chem. Chem. Phys.* **2013**, *15*, 15333-15338.
- 1266 (37) Holten-Andersen, N.; Harrington, M. J.; Birkedal, H.; Lee, B. P.; Messersmith, P. B.;  
1267 Lee, K. Y.; Waite, J. H. pH-induced metal-ligand cross-links inspired by mussel yield self-  
1268 healing polymer networks with near-covalent elastic moduli. *Proc. Natl. Acad. Sci. U. S.*  
1269 *A.* **2011**, *108*, 2651-2655.
- 1270 (38) Fullenkamp, D. E.; He, L.; Barrett, D. G.; Burghardt, W. R.; Messersmith, P. B.  
1271 Mussel-inspired histidine-based transient network metal coordination hydrogels.  
1272 *Macromolecules* **2013**, *46*, 1167-1174.
- 1273 (39) Sun, T. L.; Luo, F.; Kurokawa, T.; Karobi, S. N.; Nakajima, T.; Gong, J. P. Molecular  
1274 structure of self-healing polyampholyte hydrogels analyzed from tensile behaviors. *Soft*  
1275 *Matter* **2015**, *11*, 9355-9366.
- 1276 (40) Rosales, A. M.; Vega, S. L.; DelRio, F. W.; Burdick, J. A.; Anseth, K. S. Hydrogels  
1277 with Reversible Mechanics to Probe Dynamic Cell Microenvironments. *Angew. Chem. Int.*  
1278 *Ed.* **2017**, *56*, 12132-12136.
- 1279 (41) Liu, A.; Gao, X.; Xie, X.; Ma, W.; Xie, M.; Sun, R. Stiffness switchable  
1280 supramolecular hydrogels by photo-regulating crosslinking status. *Dyes Pigm.* **2020**, *177*,  
1281 108288.
- 1282 (42) Gandavarapu, N. R.; Azagarsamy, M. A.; Anseth, K. S. Photo-Click Living Strategy  
1283 for Controlled, Reversible Exchange of Biochemical Ligands. *Adv. Mater.* **2014**, *26*, 2521-  
1284 2526.
- 1285 (43) Li, L.; Scheiger, J. M.; Levkin, P. A. Design and Applications of Photoresponsive  
1286 Hydrogels. *Adv. Mater.* **2019**, *31*, 1807333.
- 1287 (44) Iwaso, K.; Takashima, Y.; Harada, A. Fast response dry-type artificial molecular  
1288 muscles with [c2]daisy chains. *Nat. Chem.* **2016**, *8*, 625-632.
- 1289 (45) Liu, G.; Yuan, Q.; Hollett, G.; Zhao, W.; Kang, Y.; Wu, J. Cyclodextrin-based host-  
1290 guest supramolecular hydrogel and its application in biomedical fields. *Polym. Chem.* **2018**,  
1291 *9*, 3436-3449.

- 1292 (46) Lake, G.; Thomas, A. The Strength of Highly Elastic Materials. *Proc. Math. Phys.*  
1293 *Eng. Sci.* **1967**, *300*, 108-119.
- 1294 (47) English, A. E.; Mafé, S.; Manzanares, J. A.; Yu, X.; Grosberg, A. Y.; Tanaka, T.  
1295 Equilibrium swelling properties of polyampholytic hydrogels. *J. Chem. Phys.* **1996**, *104*,  
1296 8713-8720.
- 1297 (48) Sato Matsuo, E.; Tanaka, T. Kinetics of discontinuous volume–phase transition of gels.  
1298 *J. Chem. Phys.* **1988**, *89*, 1695-1703.
- 1299 (49) Cheng, S. Z. D. Chapter 1 - Introduction. In *Phase Transitions in Polymers*; Cheng, S.  
1300 Z. D., Ed.; Elsevier: Amsterdam, 2008; pp 1-15.
- 1301 (50) Shibayama, M.; Tanaka, T. Volume phase transition and related phenomena of polymer  
1302 gels. In *Responsive Gels: Volume Transitions I*; Dušek, K., Ed.; Springer Berlin Heidelberg:  
1303 Berlin, Heidelberg, 1993; pp 1-62.
- 1304 (51) Sato, K.; Nakajima, T.; Hisamatsu, T.; Nonoyama, T.; Kurokawa, T.; Gong, J. P. Phase-  
1305 Separation-Induced Anomalous Stiffening, Toughening, and Self-Healing of  
1306 Polyacrylamide Gels. *Adv. Mater.* **2015**, *27*, 6990-6998.
- 1307 (52) Tang, J. D.; Li, C. H.; Li, H. M.; Lv, Z. Y.; Sheng, H.; Lu, T. Q.; Wang, T. J. Phase-  
1308 separation induced extraordinary toughening of magnetic hydrogels. *J. Appl. Phys.* **2018**,  
1309 *123*, 185105.
- 1310 (53) Liu, Q.; Li, S.; Zhang, P.; Lan, Y.; Lu, M. Facile preparation of PNIPAM gel with  
1311 improved deswelling kinetics by using 1-dodecanethiol as chain transfer agent. *J. Polym.*  
1312 *Res.* **2007**, *14*, 397-400.
- 1313 (54) Guo, H.; Nakajima, T.; Hourdet, D.; Marcellan, A.; Creton, C.; Hong, W.; Kurokawa,  
1314 T.; Gong, J. P. Hydrophobic Hydrogels with Fruit-Like Structure and Functions. *Adv. Mater.*  
1315 **2019**, *31*, 1900702.
- 1316 (55) Mitsumata, T.; Honda, A.; Kanazawa, H.; Kawai, M. Magnetically tunable elasticity  
1317 for magnetic hydrogels consisting of carrageenan and carbonyl iron particles. *J. Phys.*  
1318 *Chem. B* **2012**, *116*, 12341-8.
- 1319 (56) C J Whiting, A. M. V., P D Olmsted, T C B McLeish. Shear modulus of polyelectrolyte  
1320 gels under electric field. *J. Phys.: Condens. Matter* **2001**, *13*, 1381-1393.
- 1321 (57) Tungkavet, T.; Pattavarakorn, D.; Sirivat, A. Bio-compatible gelatins (Ala-Gly-Pro-  
1322 Arg-Gly-Glu-4Hyp-Gly-Pro-) and electromechanical properties: effects of temperature and  
1323 electric field. *J. Polym. Res.* **2011**, *19*, 9759.
- 1324 (58) Hirotsu, S. Electric-Field-Induced Phase Transition in Polymer. *Jpn. J. Appl. Phys.*  
1325 **1985**, *24*, 396-388.
- 1326 (59) Boustta, M.; Colombo, P. E.; Lenglet, S.; Poujol, S.; Vert, M. Versatile UCST-based  
1327 thermoresponsive hydrogels for loco-regional sustained drug delivery. *J. Control. Release*  
1328 **2014**, *174*, 1-6.
- 1329 (60) Aseyev, V.; Tenhu, H.; Winnik, F. Non-ionic Thermoresponsive Polymers in Water. In

- 1330 *Self Organized Nanostructures of Amphiphilic Block Copolymers II*; Müller, A. H. E.;  
1331 Borisov, O., Eds.; Springer Berlin Heidelberg: 2011; Chapter 57, pp 29-89.
- 1332 (61) Scarpa, J. S.; Mueller, D. D.; Klotz, I. M. Slow hydrogen-deuterium exchange in a  
1333 non- $\alpha$ -helical polyamide. *J. Am. Chem. Soc.* **1967**, *89*, 6024-6030.
- 1334 (62) Lutz, J.-F.; Akdemir, Ö.; Hoth, A. Point by Point Comparison of Two Thermosensitive  
1335 Polymers Exhibiting a Similar LCST: Is the Age of Poly(NIPAM) Over? *J. Am. Chem. Soc.*  
1336 **2006**, *128*, 13046-13047.
- 1337 (63) Takigawa, T.; Yamawaki, T.; Takahashi, K.; Masuda, T. Change in Young's modulus  
1338 of poly(N-isopropylacrylamide) gels by volume phase transition. *Polymer Gels and*  
1339 *Networks* **1998**, *5*, 585-589.
- 1340 (64) Puleo, G. L.; Zulli, F.; Piovanelli, M.; Giordano, M.; Mazzolai, B.; Beccai, L.;  
1341 Andreozzi, L. Mechanical and rheological behavior of pNIPAAm crosslinked  
1342 macrohydrogel. *React. Funct. Polym.* **2013**, *73*, 1306-1318.
- 1343 (65) Gundogan, N.; Melekaslan, D.; Okay, O. Rubber elasticity of poly(N-  
1344 isopropylacrylamide) gels at various charge densities. *Macromolecules* **2002**, *35*, 5616-  
1345 5622.
- 1346 (66) Matzelle, T. R.; Geuskens, G.; Kruse, N. Elastic Properties of Poly(N-  
1347 isopropylacrylamide) and Poly(acrylamide) Hydrogels Studied by Scanning Force  
1348 Microscopy. *Macromolecules* **2003**, *36*, 2926-2931.
- 1349 (67) Dragan, E. S. Design and applications of interpenetrating polymer network hydrogels.  
1350 A review. *Chem. Eng. J.* **2014**, *243*, 572-590.
- 1351 (68) Li, Z.; Shen, J.; Ma, H.; Lu, X.; Shi, M.; Li, N.; Ye, M. Preparation and characterization  
1352 of pH- and temperature-responsive nanocomposite double network hydrogels. *Mater. Sci.*  
1353 *Eng. C* **2013**, *33*, 1951-1957.
- 1354 (69) Fei, R.; George, J. T.; Park, J.; Grunlan, M. A. Thermoresponsive nanocomposite  
1355 double network hydrogels. *Soft Matter* **2012**, *8*, 481-487.
- 1356 (70) Fei, R.; George, J. T.; Park, J.; Means, A. K.; Grunlan, M. A. Ultra-strong  
1357 thermoresponsive double network hydrogels. *Soft Matter* **2013**, *9*, 2912.
- 1358 (71) Zheng, W. J.; An, N.; Yang, J. H.; Zhou, J.; Chen, Y. M. Tough Al-alginate/Poly(N-  
1359 isopropylacrylamide) Hydrogel with Tunable LCST for Soft Robotics. *ACS Appl. Mater.*  
1360 *Interfaces* **2015**, *7*, 1758-1764.
- 1361 (72) Haraguchi, K.; Takehisa, T.; Fan, S. Effects of clay content on the properties of  
1362 nanocomposite hydrogels composed of poly(N-isopropylacrylamide) and clay.  
1363 *Macromolecules* **2002**, *35*, 10162-10171.
- 1364 (73) Du, H.; Wickramasinghe, R.; Qian, X. Effects of salt on the lower critical solution  
1365 temperature of poly (N-isopropylacrylamide). *J. Phys. Chem. B* **2010**, *114*, 16594-16604.
- 1366 (74) Guo, H.; Brûlet, A.; Rajamohanam, P. R.; Marcellan, A.; Sanson, N.; Hourdet, D.  
1367 Influence of topology of LCST-based graft copolymers on responsive assembling in

- 1368 aqueous media. *Polymer* **2015**, *60*, 164-175.
- 1369 (75) Halperin, A.; Kröger, M.; Winnik, F. M. Poly(N-isopropylacrylamide) Phase  
1370 Diagrams: Fifty Years of Research. *Angew. Chem. Int. Ed.* **2015**, *54*, 15342-15367.
- 1371 (76) Haq, M. A.; Su, Y.; Wang, D. Mechanical properties of PNIPAM based hydrogels: A  
1372 review. *Mater. Sci. Eng. C* **2017**, *70*, 842-855.
- 1373 (77) Guo, H.; Mussault, C.; Brûlet, A.; Marcellan, A.; Hourdet, D.; Sanson, N.  
1374 Thermo-responsive Toughening in LCST-Type Hydrogels with Opposite Topology: From  
1375 Structure to Fracture Properties. *Macromolecules* **2016**, *49*, 4295-4306.
- 1376 (78) Guo, H.; Sanson, N.; Marcellan, A.; Hourdet, D. Thermo-responsive Toughening in  
1377 LCST-Type Hydrogels: Comparison between Semi-Interpenetrated and Grafted Networks.  
1378 *Macromolecules* **2016**, *49*, 9568-9577.
- 1379 (79) Mussault, C.; Guo, H.; Sanson, N.; Hourdet, D.; Marcellan, A. Effect of responsive  
1380 graft length on mechanical toughening and transparency in microphase-separated  
1381 hydrogels. *Soft Matter* **2019**, *15*, 8653-8666.
- 1382 (80) Rose, S.; Prevoteau, A.; Elziere, P.; Hourdet, D.; Marcellan, A.; Leibler, L.  
1383 Nanoparticle solutions as adhesives for gels and biological tissues. *Nature* **2014**, *505*, 382-  
1384 5.
- 1385 (81) Ida, S.; Morimura, M.; Kitanaka, H.; Hirokawa, Y.; Kanaoka, S. Swelling and  
1386 mechanical properties of thermo-responsive/hydrophilic conetworks with crosslinked  
1387 domain structures prepared from various triblock precursors. *Polym. Chem.* **2019**, *10*,  
1388 6122-6130.
- 1389 (82) Ida, S.; Kitanaka, H.; Ishikawa, T.; Kanaoka, S.; Hirokawa, Y. Swelling properties of  
1390 thermo-responsive/hydrophilic co-networks with functional crosslinked domain structures.  
1391 *Polym. Chem.* **2018**, *9*, 1701-1709.
- 1392 (83) Ida, S.; Katsurada, A.; Yoshida, R.; Hirokawa, Y. Effect of reaction conditions on  
1393 poly( N -isopropylacrylamide) gels synthesized by post-polymerization crosslinking  
1394 system. *React. Funct. Polym.* **2017**, *115*, 73-80.
- 1395 (84) Ida, S.; Katsurada, A.; Tsujio, M.; Nakamura, M.; Hirokawa, Y. Crosslinker-Based  
1396 Regulation of Swelling Behavior of Poly(N-isopropylacrylamide) Gels in a Post-  
1397 Polymerization Crosslinking System. *Gels* **2019**, *6*, 2.
- 1398 (85) Morimura, M.; Ida, S.; Oyama, M.; Takeshita, H.; Kanaoka, S. Design of Hydrogels  
1399 with Thermo-responsive Crosslinked Domain Structures via the Polymerization-Induced  
1400 Self-Assembly Process and Their Thermo-responsive Toughening in Air. *Macromolecules*  
1401 **2021**.
- 1402 (86) Wang, X.; Qiu, X.; Wu, C. Comparison of the coil-to-globule and the globule-to-coil  
1403 transitions of a single poly (N-isopropylacrylamide) homopolymer chain in water.  
1404 *Macromolecules* **1998**, *31*, 2972-2976.
- 1405 (87) Guo, H.; Sanson, N.; Hourdet, D.; Marcellan, A. Thermo-responsive Toughening with  
1406 Crack Bifurcation in Phase-Separated Hydrogels under Isochoric Conditions. *Adv. Mater.*

- 1407 **2016**, 28, 5857-64.
- 1408 (88) Kureha, T.; Hayashi, K.; Li, X.; Shibayama, M. Mechanical properties of temperature-  
1409 responsive gels containing ethylene glycol in their side chains. *Soft Matter* **2020**, 16,  
1410 10946-10953.
- 1411 (89) Seuring, J.; Agarwal, S. Polymers with upper critical solution temperature in aqueous  
1412 solution. *Macromol. Rapid Commun.* **2012**, 33, 1898-920.
- 1413 (90) Wang, K.; Liu, Q.; Liu, G.; Zeng, Y. Novel thermoresponsive homopolymers of  
1414 poly[oligo(ethylene glycol) (acyloxy) methacrylate]s: LCST-type transition in water and  
1415 UCST-type transition in alcohols. *Polymer* **2020**, 203, 122746.
- 1416 (91) Haas, H. C.; Moreau, R. D.; Schuler, N. W. Synthetic thermally reversible gel systems.  
1417 II. *Journal of Polymer Science Part A - 2: Polym. Phys.* **1967**, 5, 915-927.
- 1418 (92) Dai, X.; Zhang, Y.; Gao, L.; Bai, T.; Wang, W.; Cui, Y.; Liu, W. A Mechanically Strong,  
1419 Highly Stable, Thermoplastic, and Self-Healable Supramolecular Polymer Hydrogel. *Adv.*  
1420 *Mater.* **2015**, 27, 3566-3571.
- 1421 (93) Guo, H.; Mussault, C.; Marcellan, A.; Hourdet, D.; Sanson, N. Hydrogels with Dual  
1422 Thermoresponsive Mechanical Performance. *Macromol. Rapid Commun.* **2017**, 38,  
1423 1700287.
- 1424 (94) Ning, J.; Li, G.; Haraguchi, K. Synthesis of Highly Stretchable, Mechanically Tough,  
1425 Zwitterionic Sulfobetaine Nanocomposite Gels with Controlled Thermosensitivities.  
1426 *Macromolecules* **2013**, 46, 5317-5328.
- 1427 (95) Ren, Y.; Zhang, Y.; Sun, W.; Gao, F.; Fu, W.; Wu, P.; Liu, W. Methyl matters: An  
1428 autonomic rapid self-healing supramolecular poly(N-methacryloyl glycinamide) hydrogel.  
1429 *Polymer* **2017**, 126, 1-8.
- 1430 (96) Ge, S. J.; Li, J. J.; Geng, J.; Liu, S. N.; Xu, H.; Gu, Z. Z. Adjustable dual temperature-  
1431 sensitive hydrogel based on a self-assembly cross-linking strategy with highly stretchable  
1432 and healable properties. *Mater. Horizons* **2021**, 8, 1189-1198.
- 1433 (97) Chen, F.; Chen, Q.; Zhu, L.; Tang, Z.; Li, Q.; Qin, G.; Yang, J.; Zhang, Y.; Ren, B.;  
1434 Zheng, J. General Strategy To Fabricate Strong and Tough Low-Molecular-Weight Gelator-  
1435 Based Supramolecular Hydrogels with Double Network Structure. *Chem. Mater.* **2018**, 30,  
1436 1743-1754.
- 1437 (98) Chen, Q.; Zhu, L.; Chen, H.; Yan, H.; Huang, L.; Yang, J.; Zheng, J. A Novel Design  
1438 Strategy for Fully Physically Linked Double Network Hydrogels with Tough, Fatigue  
1439 Resistant, and Self-Healing Properties. *Adv. Funct. Mater.* **2015**, 25, 1598-1607.
- 1440 (99) Chen, Q.; Zhu, L.; Zhao, C.; Wang, Q.; Zheng, J. A Robust, One-Pot Synthesis of  
1441 Highly Mechanical and Recoverable Double Network Hydrogels Using Thermoreversible  
1442 Sol-Gel Polysaccharide. *Adv. Mater.* **2013**, 25, 4171-4176.
- 1443 (100) Van Hoorick, J.; Gruber, P.; Markovic, M.; Tromayer, M.; Van Erps, J.; Thienpont,  
1444 H.; Liska, R.; Ovsianikov, A.; Dubruel, P.; Van Vlierberghe, S. Cross-Linkable Gelatins  
1445 with Superior Mechanical Properties Through Carboxylic Acid Modification: Increasing

- 1446 the Two-Photon Polymerization Potential. *Biomacromolecules* **2017**, *18*, 3260-3272.
- 1447 (101) Mallick, P. K. 5 - Thermoplastics and thermoplastic–matrix composites for  
1448 lightweight automotive structures. In *Materials, Design and Manufacturing for*  
1449 *Lightweight Vehicles*; Mallick, P. K., Ed.; Woodhead Publishing: 2010; pp 174-207.
- 1450 (102) Wang, Y. J.; Zhang, X. N.; Song, Y.; Zhao, Y.; Chen, L.; Su, F.; Li, L.; Wu, Z. L.;  
1451 Zheng, Q. Ultrastiff and Tough Supramolecular Hydrogels with a Dense and Robust  
1452 Hydrogen Bond Network. *Chem. Mater.* **2019**, *31*, 1430-1440.
- 1453 (103) Zhang, X. N.; Du, C.; Du, M.; Zheng, Q.; Wu, Z. L. Kinetic insights into glassy  
1454 hydrogels with hydrogen bond complexes as the cross-links. *Materials Today Physics* **2020**,  
1455 *15*, 100230.
- 1456 (104) Jiao, C.; Chen, Y.; Liu, T.; Peng, X.; Zhao, Y.; Zhang, J.; Wu, Y.; Wang, H. Rigid and  
1457 Strong Thermoresponsive Shape Memory Hydrogels Transformed from  
1458 Poly(vinylpyrrolidone-co-acryloxy acetophenone) Organogels. *ACS Appl. Mater.*  
1459 *Interfaces* **2018**, *10*, 32707-32716.
- 1460 (105) Mredha, M. T. I.; Pathak, S. K.; Tran, V. T.; Cui, J.; Jeon, I. Hydrogels with Superior  
1461 Mechanical Properties from the Synergistic Effect in Hydrophobic–Hydrophilic  
1462 Copolymers. *Chem. Eng. J.* **2019**, *362*, 325-338.
- 1463 (106) Wang, F.; Weiss, R. A. Thermoresponsive Supramolecular Hydrogels with High  
1464 Fracture Toughness. *Macromolecules* **2018**, *51*, 7386-7395.
- 1465 (107) Luo, F.; Sun, T. L.; Nakajima, T.; Kurokawa, T.; Li, X.; Guo, H.; Huang, Y.; Zhang,  
1466 H.; Gong, J. P. Tough Polyion-Complex Hydrogels from Soft to Stiff Controlled by  
1467 Monomer Structure. *Polymer* **2017**, *116*, 487-497.
- 1468 (108) Ihsan, A. B.; Sun, T. L.; Kurokawa, T.; Karobi, S. N.; Nakajima, T.; Nonoyama, T.;  
1469 Roy, C. K.; Luo, F.; Gong, J. P. Self-Healing Behaviors of Tough Polyampholyte Hydrogels.  
1470 *Macromolecules* **2016**, *49*, 4245-4252.
- 1471 (109) Luo, F.; Sun, T. L.; Nakajima, T.; King, D. R.; Kurokawa, T.; Zhao, Y.; Ihsan, A. B.;  
1472 Li, X.; Guo, H.; Gong, J. P. Strong and Tough Polyion-Complex Hydrogels from  
1473 Oppositely Charged Polyelectrolytes: A Comparative Study with Polyampholyte  
1474 Hydrogels. *Macromolecules* **2016**, *49*, 2750-2760.
- 1475 (110) Liu, B.; Xu, Z.; Gao, H.; Fan, C.; Ma, G.; Zhang, D.; Xiao, M.; Zhang, B.; Yang, Y.;  
1476 Cui, C.; Wu, T.; Feng, X.; Liu, W. Stiffness Self-Tuned Shape Memory Hydrogels for  
1477 Embolization of Aneurysm. *Adv. Funct. Mater.* **2020**, *30*, 1910197.
- 1478 (111) Berthier, L.; Biroli, G. Theoretical perspective on the glass transition and amorphous  
1479 materials. *Rev.Mod. Phys.* **2011**, *83*, 587-645.
- 1480 (112) Liang, R.; Yu, H.; Wang, L.; Lin, L.; Wang, N.; Naveed, K. U. Highly Tough  
1481 Hydrogels with the Body Temperature-Responsive Shape Memory Effect. *ACS Appl. Mater.*  
1482 *Interfaces* **2019**, *11*, 43563-43572.
- 1483 (113) Matsuda, A.; Sato, J. i.; Yasunaga, H.; Osada, Y. Order-Disorder Transition of a  
1484 Hydrogel Containing an n-Alkyl Acrylate. *Macromolecules* **1994**, *27*, 7695-7698.

- 1485 (114) Osada, Y.; Matsuda, A. Shape memory in hydrogels. *Nature* **1995**, *376*, 219.
- 1486 (115) Bilici, C.; Can, V.; Nöchel, U.; Behl, M.; Lendlein, A.; Okay, O. Melt-Processable  
1487 Shape-Memory Hydrogels with Self-Healing Ability of High Mechanical Strength.  
1488 *Macromolecules* **2016**, *49*, 7442-7449.
- 1489 (116) Zhang, K.; Zhao, Z.; Huang, J.; Zhao, T.; Fang, R.; Liu, M. Self-recoverable semi-  
1490 crystalline hydrogels with thermomechanics and shape memory performance. *Sci. China*  
1491 *Mater.* **2018**, *62*, 586-596.
- 1492 (117) Tuncaboylu, D. C.; Argun, A.; Sahin, M.; Sari, M.; Okay, O. Structure optimization  
1493 of self-healing hydrogels formed via hydrophobic interactions. *Polymer* **2012**, *53*, 5513-  
1494 5522.
- 1495 (118) Kurt, B.; Gulyuz, U.; Demir, D. D.; Okay, O. High-strength semi-crystalline  
1496 hydrogels with self-healing and shape memory functions. *Eur. Polym. J.* **2016**, *81*, 12-23.
- 1497 (119) Bilici, C.; Okay, O. Shape Memory Hydrogels via Micellar Copolymerization of  
1498 Acrylic Acid and n-Octadecyl Acrylate in Aqueous Media. *Macromolecules* **2013**, *46*,  
1499 3125-3131.
- 1500 (120) Miyazaki, T.; Kaneko, T.; Gong, J. P.; Osada, Y.; Demura, M.; Suzuki, M. Water-  
1501 Induced Crystallization of Hydrogels. *Langmuir* **2002**, *18*, 965-967.
- 1502 (121) Okay, O. Semicrystalline physical hydrogels with shape-memory and self-healing  
1503 properties. *J. Mater. Chem. B* **2019**, *7*, 1581-1596.
- 1504 (122) ACS Appl Mater Interfaces Zhao, Z.; Liu, Y.; Zhang, K.; Zhuo, S.; Fang, R.; Zhang,  
1505 J.; Jiang, L.; Liu, M. Biphasic Synergistic Gel Materials with Switchable Mechanics and  
1506 Self-Healing Capacity. *Angew. Chem. Int. Ed.* **2017**, *56*, 13464-13469.
- 1507 (123) Zhao, Z.; Zhang, K.; Liu, Y.; Zhou, J.; Liu, M. Highly Stretchable, Shape Memory  
1508 Organohydrogels Using Phase-Transition Microinclusions. *Adv. Mater.* **2017**, *29*, 1701695.
- 1509 (124) Zhao, Z.; Zhuo, S.; Fang, R.; Zhang, L.; Zhou, X.; Xu, Y.; Zhang, J.; Dong, Z.; Jiang,  
1510 L.; Liu, M. Dual-Programmable Shape-Morphing and Self-Healing Organohydrogels  
1511 Through Orthogonal Supramolecular Heteronetworks. *Adv. Mater.* **2018**, *30*, 1804435.
- 1512 (125) Li, L.; Scheiger, J. M.; Levkin, P. A. Design and Applications of Photoresponsive  
1513 Hydrogels. *Adv. Mater.* **2019**, *31*, 1807333.
- 1514 (126) Tao, Z.; Fan, H.; Huang, J.; Sun, T.; Kurokawa, T.; Gong, J. P. Fabrication of Tough  
1515 Hydrogel Composites from Photoresponsive Polymers to Show Double-Network Effect.  
1516 *ACS Appl. Mater. Interfaces* **2019**, *11*, 37139-37146.
- 1517 (127) Moorthy, J. N.; Venkatesan, K.; Weiss, R. G. Photodimerization of Coumarins in  
1518 Solid Cyclodextrin Inclusion Complexes. *J. Org. Chem.* **1992**, *57*, 3292-3297.
- 1519 (128) Ma, Y.; Hua, M.; Wu, S.; Du, Y.; Pei, X.; Zhu, X.; Zhou, F.; He, X. Bioinspired high-  
1520 power-density strong contractile hydrogel by programmable elastic recoil. *Sci. Adv.* **2020**,  
1521 *6*, eabd2520.
- 1522 (129) Gao, Y.; Wu, K.; Suo, Z. Photodetachable Adhesion. *Adv. Mater.* **2019**, *31*, 1806948.

- 1523 (130) Guvendiren, M.; Burdick, J. A. Stiffening hydrogels to probe short- and long-term  
1524 cellular responses to dynamic mechanics. *Nat. Commun.* **2012**, *3*, 792.
- 1525 (131) Rowlands, A. S.; George, P. A.; Cooper-White, J. J. Directing osteogenic and  
1526 myogenic differentiation of MSCs: interplay of stiffness and adhesive ligand presentation.  
1527 *Am. J. Physiol., Cell Physiol.* **2008**, *295*, C1037-C1044.
- 1528 (132) Lee, I. N.; Dobre, O.; Richards, D.; Ballestrom, C.; Curran, J. M.; Hunt, J. A.;  
1529 Richardson, S. M.; Swift, J.; Wong, L. S. Photoresponsive Hydrogels with Photoswitchable  
1530 Mechanical Properties Allow Time-Resolved Analysis of Cellular Responses to Matrix  
1531 Stiffening. *ACS Appl. Mater. Interfaces* **2018**, *10*, 7765-7776.
- 1532 (133) Rosales, A. M.; Mabry, K. M.; Nehls, E. M.; Anseth, K. S. Photoresponsive Elastic  
1533 Properties of Azobenzene-Containing Poly(ethylene-glycol)-Based Hydrogels.  
1534 *Biomacromolecules* **2015**, *16*, 798-806.
- 1535 (134) Yang, X.; Liu, X.; Liu, Z.; Pu, F.; Ren, J.; Qu, X. Near-infrared light-triggered,  
1536 targeted drug delivery to cancer cells by aptamer gated nanovehicles. *Adv. Mater.* **2012**, *24*,  
1537 2890-2895.
- 1538 (135) Fujigaya, T.; Morimoto, T.; Niidome, Y.; Nakashima, N. NIR Laser-Driven  
1539 Reversible Volume Phase Transition of Single-Walled Carbon Nanotube/Poly(N-  
1540 isopropylacrylamide) Composite Gels. *Adv. Mater.* **2008**, *20*, 3610-3614.
- 1541 (136) Zhu, C. H.; Lu, Y.; Chen, J. F.; Yu, S. H. Photothermal poly(N-  
1542 isopropylacrylamide)/Fe<sub>3</sub>O<sub>4</sub> nanocomposite hydrogel as a movable position heating  
1543 source under remote control. *Small* **2014**, *10*, 2796-2800.
- 1544 (137) Li, W.; Wang, J.; Ren, J.; Qu, X. 3D Graphene Oxide–Polymer Hydrogel: Near-  
1545 Infrared Light-Triggered Active Scaffold for Reversible Cell Capture and On-Demand  
1546 Release. *Adv. Mater.* **2013**, *25*, 6737-6743.
- 1547 (138) Huang, J.; Zhao, L.; Wang, T.; Sun, W.; Tong, Z. NIR-Triggered Rapid Shape  
1548 Memory PAM-GO-Gelatin Hydrogels with High Mechanical Strength. *ACS Appl. Mater.*  
1549 *Interfaces* **2016**, *8*, 12384-12392.
- 1550 (139) Dai, C. F.; Zhang, X. N.; Du, C.; Frank, A.; Schmidt, H. W.; Zheng, Q.; Wu, Z. L.  
1551 Photoregulated Gradient Structure and Programmable Mechanical Performances of Tough  
1552 Hydrogels with a Hydrogen-Bond Network. *ACS Appl. Mater. Interfaces* **2020**, *12*, 53376-  
1553 53384.
- 1554 (140) Dai, C. F.; Du, C.; Xue, Y.; Zhang, X. N.; Zheng, S. Y.; Liu, K.; Wu, Z. L.; Zheng, Q.  
1555 Photodirected Morphing Structures of Nanocomposite Shape Memory Hydrogel with High  
1556 Stiffness and Toughness. *ACS Appl. Mater. Interfaces* **2019**, *11*, 43631-43640.
- 1557 (141) Ryplida, B.; Lee, K. D.; In, I.; Park, S. Y. Light - Induced Swelling - Responsive  
1558 Conductive, Adhesive, and Stretchable Wireless Film Hydrogel as Electronic Artificial  
1559 Skin. *Adv. Funct. Mater.* **2019**, *29*, 1903209.
- 1560 (142) Hua, L.; Xie, M.; Jian, Y.; Wu, B.; Chen, C.; Zhao, C. Multiple-Responsive and  
1561 Amphibious Hydrogel Actuator Based on Asymmetric UCST-Type Volume Phase

- 1562 Transition. *ACS Appl. Mater. Interfaces* **2019**, *11*, 43641-43648.
- 1563 (143) Scheiger, J. M.; Levkin, P. A. Hydrogels with Preprogrammable Lifetime via UV-  
1564 Induced Polymerization and Degradation. *Adv. Funct. Mater.* **2020**, *30*, 1909800.
- 1565 (144) Koetting, M. C.; Peters, J. T.; Steichen, S. D.; Peppas, N. A. Stimulus-responsive  
1566 hydrogels: Theory, modern advances, and applications. *Mater. Sci. Eng. R Rep.* **2015**, *93*,  
1567 1-49.
- 1568 (145) Steiner, T. The Hydrogen Bond in the Solid State. *Angew. Chem. Int. Ed.* **2002**, *41*,  
1569 48-76.
- 1570 (146) Gao, F.; Zhang, Y.; Li, Y.; Xu, B.; Cao, Z.; Liu, W. Sea Cucumber-Inspired Autolytic  
1571 Hydrogels Exhibiting Tunable High Mechanical Performances, Repairability, and  
1572 Reusability. *ACS Appl. Mater. Interfaces* **2016**, *8*, 8956-66.
- 1573 (147) Wang, Y. J.; Li, C. Y.; Wang, Z. J.; Zhao, Y.; Chen, L.; Wu, Z. L.; Zheng, Q. Hydrogen  
1574 bond-reinforced double-network hydrogels with ultrahigh elastic modulus and shape  
1575 memory property. *J. Polym. Sci., Part B: Polym. Phys.* **2018**, *56*, 1281-1286.
- 1576 (148) Ding, H.; Zhang, X. N.; Zheng, S. Y.; Song, Y.; Wu, Z. L.; Zheng, Q. Hydrogen bond  
1577 reinforced poly(1-vinylimidazole-co-acrylic acid) hydrogels with high toughness, fast self-  
1578 recovery, and dual pH-responsiveness. *Polymer* **2017**, *131*, 95-103.
- 1579 (149) Zhang, X. N.; Wang, Y. J.; Sun, S.; Hou, L.; Wu, P.; Wu, Z. L.; Zheng, Q. A Tough  
1580 and Stiff Hydrogel with Tunable Water Content and Mechanical Properties Based on the  
1581 Synergistic Effect of Hydrogen Bonding and Hydrophobic Interaction. *Macromolecules*  
1582 **2018**, *51*, 8136-8146.
- 1583 (150) Li, X.; Li, R.; Liu, Z.; Gao, X.; Long, S.; Zhang, G. Integrated Functional High-  
1584 Strength Hydrogels with Metal-Coordination Complexes and H-Bonding Dual Physically  
1585 Cross-linked Networks. *Macromol. Rapid Commun.* **2018**, *39*, 1800400.
- 1586 (151) Yu, H. C.; Li, C. Y.; Du, M.; Song, Y.; Wu, Z. L.; Zheng, Q. Improved Toughness and  
1587 Stability of  $\kappa$ -Carrageenan/Polyacrylamide Double-Network Hydrogels by Dual Cross-  
1588 Linking of the First Network. *Macromolecules* **2019**, *52*, 629-638.
- 1589 (152) Das Mahapatra, R.; Imani, K. B. C.; Yoon, J. Integration of Macro-Cross-Linker and  
1590 Metal Coordination: A Super Stretchable Hydrogel with High Toughness. *ACS Appl. Mater.*  
1591 *Interfaces* **2020**, *12*, 40786-40793.
- 1592 (153) Cao, J.; Li, J.; Chen, Y.; Zhang, L.; Zhou, J. Dual Physical Crosslinking Strategy to  
1593 Construct Moldable Hydrogels with Ultrahigh Strength and Toughness. *Adv. Funct. Mater.*  
1594 **2018**, *28*, 1800739.
- 1595 (154) Henderson, K. J.; Zhou, T. C.; Otim, K. J.; Shull, K. R. Ionically Cross-Linked  
1596 Triblock Copolymer Hydrogels with High Strength. *Macromolecules* **2010**, *43*, 6193-6201.
- 1597 (155) Nisato, G.; Skouri, R.; Schosseler, F.; Munch, J.-P.; Candau, S. J. Elastic behaviour  
1598 of salt-free polyelectrolyte gels. *Faraday Discuss.* **1995**, *101*, 133-146.
- 1599 (156) Xiao, Y. Y.; Gong, X. L.; Kang, Y.; Jiang, Z. C.; Zhang, S.; Li, B. J. Light-, pH- and

1600 thermal-responsive hydrogels with the triple-shape memory effect. *Chem. Commun.* **2016**,  
1601 52, 10609-10612.

1602 (157) Li, Y.; Tanaka, T. Kinetics of swelling and shrinking of gels. *J. Chem. Phys.* **1990**,  
1603 92, 1365-1371.

1604 (158) Pearson, R. G. Hard and Soft Acids and Bases. In *Survey of Progress in Chemistry*;  
1605 Scott, A. F., Ed.; Elsevier: 1969; pp 1-52.

1606 (159) Chen, Q.; Yan, X.; Zhu, L.; Chen, H.; Jiang, B.; Wei, D.; Huang, L.; Yang, J.; Liu,  
1607 B.; Zheng, J. Improvement of Mechanical Strength and Fatigue Resistance of Double  
1608 Network Hydrogels by Ionic Coordination Interactions. *Chem. Mater.* **2016**, 28, 5710-5720.

1609 (160) Sun, J. Y.; Zhao, X.; Illeperuma, W. R.; Chaudhuri, O.; Oh, K. H.; Mooney, D. J.;  
1610 Vlassak, J. J.; Suo, Z. Highly stretchable and tough hydrogels. *Nature* **2012**, 489, 133-136.

1611 (161) Lane, D. D.; Kaur, S.; Weerasakare, G. M.; Stewart, R. J. Toughened hydrogels  
1612 inspired by aquatic caddisworm silk. *Soft Matter* **2015**, 11, 6981-90.

1613 (162) Hu, Y.; Du, Z.; Deng, X.; Wang, T.; Yang, Z.; Zhou, W.; Wang, C. Dual Physically  
1614 Cross-Linked Hydrogels with High Stretchability, Toughness, and Good Self-  
1615 Recoverability. *Macromolecules* **2016**, 49, 5660-5668.

1616 (163) Cao, J.; Wang, Y.; He, C.; Kang, Y.; Zhou, J. Ionically crosslinked  
1617 chitosan/poly(acrylic acid) hydrogels with high strength, toughness and antifreezing  
1618 capability. *Carbohydr. Polym.* **2020**, 242, 116420.

1619 (164) Li, J.; Illeperuma, W. R. K.; Suo, Z.; Vlassak, J. J. Hybrid Hydrogels with Extremely  
1620 High Stiffness and Toughness. *ACS Macro Lett.* **2014**, 3, 520-523.

1621 (165) Yu, H. C.; Zheng, S. Y.; Fang, L.; Ying, Z.; Du, M.; Wang, J.; Ren, K.-F.; Wu, Z. L.;  
1622 Zheng, Q. Reversibly Transforming a Highly Swollen Polyelectrolyte Hydrogel to an  
1623 Extremely Tough One and its Application as a Tubular Grasper. *Adv. Mater.* **2020**, 32,  
1624 2005171.

1625 (166) Baldwin, R. L. How Hofmeister ion interactions affect protein stability. *Biophys. J.*  
1626 **1996**, 71, 2056-2063.

1627 (167) Jungwirth, P.; Cremer, P. S. Beyond Hofmeister. *Nat. Chem.* **2014**, 6, 261-263.

1628 (168) Zhang, Y.; Cremer, P. S. Chemistry of Hofmeister anions and osmolytes. *Annu. Rev.*  
1629 *Phys. Chem.* **2010**, 61, 63-83.

1630 (169) Zhang, Y.; Furyk, S.; Bergbreiter, D. E.; Cremer, P. S. Specific Ion Effects on the  
1631 Water Solubility of Macromolecules: PNIPAM and the Hofmeister Series. *J. Am. Chem.*  
1632 *Soc.* **2005**, 127, 14505-14510.

1633 (170) Tuncaboylu, D. C.; Sari, M.; Oppermann, W.; Okay, O. Tough and Self-Healing  
1634 Hydrogels Formed via Hydrophobic Interactions. *Macromolecules* **2011**, 44, 4997-5005.

1635 (171) Sun, X.; Luo, C.; Luo, F. Preparation and properties of self-healable and conductive  
1636 PVA-agar hydrogel with ultra-high mechanical strength. *Eur. Polym. J.* **2020**, 124, 109465.

1637 (172) Chen, W.; Li, D.; Bu, Y.; Chen, G.; Wan, X.; Li, N. Design of strong and tough  
1638 methylcellulose-based hydrogels using kosmotropic Hofmeister salts. *Cellulose* **2019**, *27*,  
1639 1113-1126.

1640 (173) Wu, S.; Hua, M.; Alsaid, Y.; Du, Y.; Ma, Y.; Zhao, Y.; Lo, C. Y.; Wang, C.; Wu, D.;  
1641 Yao, B.; Strzalka, J.; Zhou, H.; Zhu, X.; He, X. Poly(vinyl alcohol) Hydrogels with Broad-  
1642 Range Tunable Mechanical Properties via the Hofmeister Effect. *Adv. Mater.* **2021**,  
1643 e2007829.

1644 (174) Li, P.; Wang, Z.; Lin, X.; Wang, X.; Guo, H. Muscle-Inspired Ion-Sensitive  
1645 Hydrogels with Highly Tunable Mechanical Performance for Versatile Engineering  
1646 Applications. *Sci. China Mater.* **2021**.

1647 (175) Cui, C.; Shao, C.; Meng, L.; Yang, J. High-Strength, Self-Adhesive, and Strain-  
1648 Sensitive Chitosan/Poly(acrylic acid) Double-Network Nanocomposite Hydrogels  
1649 Fabricated by Salt-Soaking Strategy for Flexible Sensors. *ACS Appl. Mater. Interfaces*  
1650 **2019**, *11*, 39228-39237.

1651 (176) Sun, T. L.; Kurokawa, T.; Kuroda, S.; Ihsan, A. B.; Akasaki, T.; Sato, K.; Haque, M.  
1652 A.; Nakajima, T.; Gong, J. P. Physical Hydrogels Composed of Polyampholytes  
1653 Demonstrate High Toughness and Viscoelasticity. *Nat. Mater.* **2013**, *12*, 932-937.

1654 (177) Luo, F.; Sun, T. L.; Nakajima, T.; Kurokawa, T.; Zhao, Y.; Sato, K.; Ihsan, A. B.; Li,  
1655 X.; Guo, H.; Gong, J. P. Oppositely charged polyelectrolytes form tough, self-healing, and  
1656 rebuildable hydrogels. *Adv. Mater.* **2015**, *27*, 2722-2727.

1657 (178) Fan, H.; Wang, J.; Tao, Z.; Huang, J.; Rao, P.; Kurokawa, T.; Gong, J. P. Adjacent  
1658 cationic-aromatic sequences yield strong electrostatic adhesion of hydrogels in seawater.  
1659 *Nat. Commun.* **2019**, *10*, 5127.

1660 (179) Means, A. K.; Grunlan, M. A. Modern Strategies To Achieve Tissue-Mimetic,  
1661 Mechanically Robust Hydrogels. *ACS Macro Lett.* **2019**, *8*, 705-713.

1662